Journal Name

RSCPublishing

ARTICLE

Cite this: DOI: 10.1039/xoxxoooooox

Received ooth January 2012,
Accepted ooth January 2012

DOI: 10.1039/xoxxoooooox

www.rsc.org/

New palladium(II) and platinum(II) 5,5-diethylbarbiturate complexes with 2-phenylpyridine, 2,2'-bipyridine and 2,2'-dipyridylamine: synthesis, structures, DNA binding, molecular docking, cellular uptake, antioxidant activity and cytotoxicity

Ceyda Icsel,[a] Veysel T. Yilmaz,*[a] Yunus Kaya,[a] Hale Samli,[b] William T. A. Harrison[c] and Orhan Buyukgungor[d]

Novel palladium(II) and platinum(II) complexes of 5,5-diethylbarbiturate (barb) with 2-phenylpyridine (Hppy), 2,2'-bipyridine (bpy) and 2,2'-dipyridylamine (dpya) have been prepared and characterized by elemental analysis, IR, UV-Vis, NMR and ESI-MS. Single-crystal diffraction measurements show that complex **1** consists of binuclear $[Pd_2(\mu\text{-barb-}\kappa N,O)_2(ppy\text{-}\kappa N,C)_2]$ moieties, while complexes **3**–**5** are mononuclear, $[M(barb\text{-}\kappa N)_2(L\text{-}\kappa N,N')]$ (L = bpy or dpya). **6** has a composition of $[Pt(dpya\text{-}\kappa N,N')_2][Ag(barb\text{-}\kappa N)_2]_2\cdot 4H_2O$ and **2** was assumed to have a structure of $[Pt(barb\text{-}\kappa N)(Hppy\text{-}\kappa N)(ppy\text{-}\kappa N,C)]\cdot 3H_2O$. The complexes were found to exhibit significant DNA binding affinity by a non-covalent binding mode, in accordance with molecular docking studies. In addition, complexes **1** and **2** displayed strong binding with supercoiled pUC19 plasmid DNA. Cellular uptake studies were performed to assess the subcellular localization of the selected complexes. A moderate radical scavenging activity of **1** and **2** was confirmed by DPPH and ABTS tests. Complexes **1**, **2**, and **5** showed selectivity against HT-29 (colon) cell line.

Introduction

Since the discovery of anticancer activity of cisplatin, *cis*-$[PtCl_2(NH_3)_2]$, in the 1970's, metal complexes have gained a progressively increasing interest in medicinal chemistry.[1-5] The more effective and less toxic second- and third-generation platinum-based anticancer agents, carboplatin and oxaliplatin with the leaving groups of 1,1-cyclobutanedicarboxylate and oxalate, respectively, were successfully tested and went on to achieve worldwide clinical acceptance.[6,7] The presence of chloride anions as leaving groups promotes DNA-binding ability of cisplatin via covalent bonding, while the carboxylate anions in carboplatin and oxaliplatin improve the water solubility and the stability of these complexes.[8-11]

DNA is the main biological target for anticancer drugs. Hence, the design and synthesis of DNA targeting metal-based anticancer agents with potential cytotoxicity have gained importance in recent years.[12,13] Metal complexes containing aromatic ligands are reported to exhibit a dual-function mode of action, in which DNA binding occurs through both coordination with the metal centre, and non-covalent interaction such as intercalation with the DNA base pairs, along with π-π aromatic interactions between the double helix and the aromatic components of the metal complex.[14-18] Moreover, some metal complexes with bulky ligands are shown to act as DNA groove binders.[19-21]

5,5-Diethylbarbituric acid (barbH), also known as barbitone, barbital, veronal or diemal, is a barbiturate derivative and is used as a sedative and hypnotic drug in the form of its soluble salt, sodium barbital.[22] The coordination chemistry of barbiturates is interesting and begins with the preparation of a crystalline copper(II) complex of 5,5-diethylbarbiturate (barb) with pyridine (py), $[Cu(barb)_2(py)_2]$.[23] Barbituric acids are weak acids and readily deprotonate in aqueous solutions, forming corresponding barbiturate anions. The donor atoms such as amine N and carbonyl O atoms make the barbiturates interesting ligands, forming metal complexes from mononuclear species to coordination polymers and supramolecular assemblies.[24] Among barbiturates, metal

complexes of barb have received much attention, probably due to its easy coordination to various metal ions.[24]

Barbiturates consist of a planar pyrimidine ring with various substituents on this basic skeleton and are structurally related to the pyrimidine nucleobases such as uracil, thymine and cytosine. The platinum(II) complexes of these bioligands, in particular those of uracil and thymine, have received considerable attention over the last three decades because of their likely relevance to the chemistry of anticancer platinum complexes, and the vast majority of the work was performed by Lippert and co-workers.[25-29] On the other hand, palladium(II) and platinum(II) complexes of barb have not been studied extensively and only a few reports on the synthesis of a number of *cis*-[PtCl(barb)$(L)_2$] complexes (L = different phosphine ligands)[30] and the crystal structures of *cis*-[PtCl(barb)$(PPh_3)_2]\cdot CH_2Cl_2$,[30] *trans*-[PtCl(barb)$(PPh_3)_2$],[31] $(Et_4N)_6[\{Pd_3(Br_3L)\}_6(\mu\text{-barb})_9]$[32] and $(Et_3NH)_4(Et_4N)_4[\{Pd_3(Br_3L)\}_4(\mu\text{-barb})_4(Hbarb)_4]$[32] appeared in the literature. The barb ligand in the platinum(II) complexes is N-coordinated, while those in the palladium(II) complexes act as a bridging ligand. Although a large number of metal complexes of barb appeared in the literature, their biological evaluation received less attention and the antimicrobial activity of a few metal complexes of barb was reported.[33-36]

Herein we report the coordination behaviour of the barb ligand towards palladium(II) and platinum(II) metal ions in the presence of three planar aromatic ligands, 2-phenylpyridine (Hppy), 2,2'-bipyridine (bpy) and 2,2'-dipyridylamine (dpya). The title complexes are shown in Scheme 1. The interaction of **1–6** with DNA was studied using various techniques. Further, the molecular docking technique was also utilized to ascertain the action mode of the complexes towards DNA. The antioxidant activity of the complexes was studied in DPPH and ABTS tests. Intracellular localisation of the complexes was determined. Cytotoxic activities were assayed against breast (MCF-7), colon (HT-29) and prostate (DU-145) cancer cell lines.

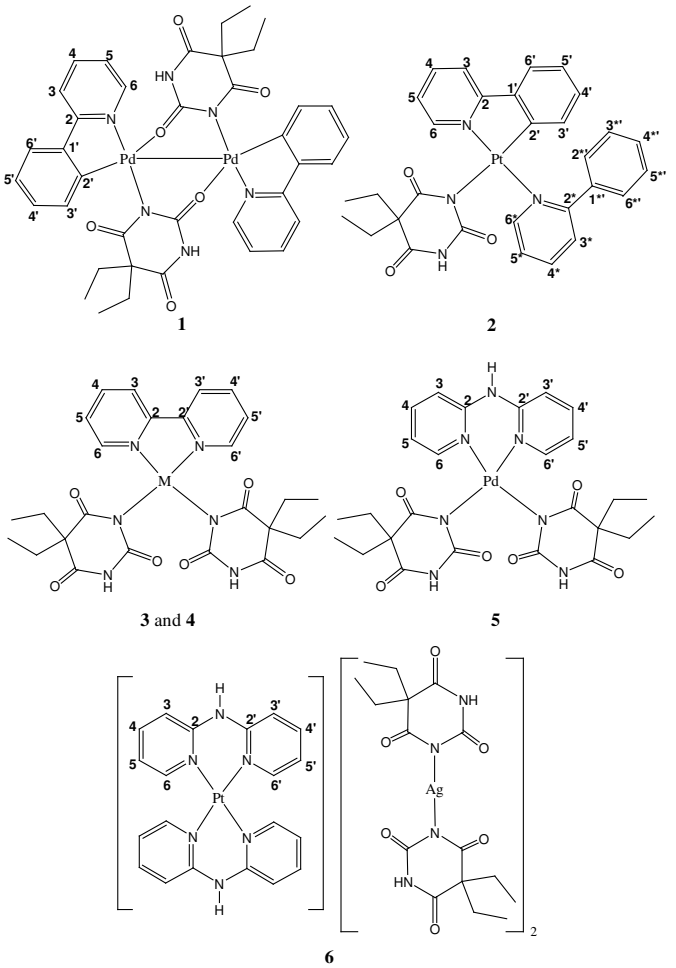

Scheme 1 A schematic representation of complexes **1–6** (M = Pd or Pt) with the atom numbering for NMR spectroscopy.

Results and discussion

Synthesis, characterization and stability studies

The reaction of Hppy with $PdCl_2$ in the presence of Na(barb) yields a binuclear complex of **1**, while the reaction with $K_2[PtCl_4]$ gives a mononuclear complex of **2**. Complexes **3–6** were prepared by the ligand displacement of barb with the chlorides in $[MCl_2(L)]$ complexes, synthesized by the methods reported earlier.[37-40] The structure of **6** is different from those of the complexes. Although the same method was used to prepare both **5** and **6**, the silver(I) ions are coordinated by barb ligands during the removal of chlorides by $AgNO_3$, leading to the formation of $[Pt(dpya)_2][Ag(barb)_2]_2$ (**6**). All these complexes were obtained in high yields of 71-91%.

The formulae of the complexes were firstly deduced from their elemental analysis and spectroscopic data, and confirmed by X-ray diffraction. Our attempts to grow X-ray quality crystals of **2** failed. However, based on elemental analysis,NMR and ESI-MS, it is assumed that it has a molecular structure of $[Pt(barb)(ppy)(Hppy)]\cdot 3H_2O$, in which Hppy acts as a monodentate ligand, while the ppy^- anion behaves as a bidentate cyclometalated ligand. Both coordination modes were observed in [Pt(ppy)(Hppy)Cl].[41] The composition of **2** is further supported by TG/DTA analysis. The TG curve of **2** displays three distinct decomposition stages in the temperature range of 98-200, 210-370, and 375-496 °C, and the corresponding mass losses agree well with the removal of three water molecules of crystallization (found 7.5%, calc. 7.3%), two molecules of ppy (found 41.2%, calc. 41.7%) and a molecule of barb (found 25.0%, calc. 24.7%) in the complex.

The title complexes are stable towards air and moisture, and are readily soluble in MeOH, EtOH and DMSO and also in the aqueous solutions of MeCN, MeOH and EtOH (H_2O:solvent = 1:1 v:v). The electrical conductivity measurements indicate that complexes **1–5** show a nonelectrolytic behaviour with Λ_M values ranging from 11 to 21 S cm^2 mol^{-1} in MeOH, and from 3 to 12 S cm^2 mol^{-1} in DMSO, while the molar conductance values of **6** are 172 and 74 S cm^2 mol^{-1} in MeOH and DMSO, respectively, suggesting its 1:2 electrolyte nature.[42]

Table 1 Crystallographic data and structure refinement for complexes **1** and **3–6**

Complexes	**1**	**3**	**4**	**5**	**6**
Empirical formula	$C_{38}H_{38}N_6O_6Pd_2$	$C_{26}H_{30}N_6O_6Pd$	$C_{26}H_{30}N_6O_6Pt$	$C_{26}H_{31}N_7O_6Pd$	$C_{52}H_{70}Ag_2N_{14}O_{16}Pt$
M	887.54	628.96	717.65	643.98	1558.05
T (K)	293(2)	120(2)	120(2)	120(2)	293(2)
Crystal system	triclinic	monoclinic	monoclinic	triclinic	triclinic
Space group	$P\bar{1}$	$P2_1/c$	$P2_1/c$	$P\bar{1}$	$P\bar{1}$
a (Å)	12.1633(6)	11.5460(2)	11.5076(3)	11.631(7)	11.0480(4)
b (Å)	13.0880(8)	22.1844(6)	22.3550(7)	12.252(9)	11.4890(4)
c (Å)	14.6045(7)	13.2450(3)	13.2889(4)	12.778(15)	12.7247(5)
α (^{o})	71.039(4)	90.00	90.00	104.54(3)	72.852(3)
β (^{o})	66.529(4)	99.2996(13)	99.2282(17)	101.15(3)	86.993(3)
γ (^{o})	87.850(5)	90.00	90.00	108.709(1)	84.128(3)
V (Å^3)	2005.52(18)	3348.00(13)	3374.36(17)	1593(2)	1534.83(10)
Z	2	4	4	2	1
ρ (calc) (g cm^{-3})	1.470	1.248	1.413	1.342	1.686
θ for data collection	1.84-26.00	3.12-27.54	3.11-27.52	1.67-26.00	1.85-26.00
Total reflections	19968	7680	7710	6459	28112
Independent reflections (R_{int})	7866 (0.0614)	6331 (0.0488)	6428 (0.0444)	4718 (0.1099)	6026 (0.0231)
Goodness of fit on F^2	0.846	1.083	1.056	1.060	0.999
R_1 [$I>2\sigma$]	0.0488	0.0482	0.0321	0.0875	0.0204
wR_2 (F^2)	0.1081	0.1170	0.0866	0.2626	0.0440

IR spectra of **1–6** display the characteristic bands of the ligands. For example, the ν(NH) vibration of the barb ligand appears at ca. 3176 cm^{-1}, while that of dpya is observed over 3300 cm^{-1}. The ν(CO) vibrations of barb are observed as the three distinct bands in the frequency range 1630-1730 cm^{-1}. The signals in the ^{1}H NMR spectra of **1–6** are assigned according to the numbering in Scheme 1. The NH proton of barb appears as a singlet in the range of δ 10.46-10.74 ppm, while the signal centered at 9.65 ppm in the spectra of **5** and **6** is attributed to the NH proton of dpya. The aromatic protons are observed as a multiplet between δ 8.96-6.81 ppm and experience deshielding compared to those of the free ligands. The signals observed in the range of 2.21-1.24 and 1.06-0.31 ppm correspond to the proton resonances of the CH_2 and CH_3 groups of barb, respectively. Moreover, the signals of ^{13}C NMR are consistent with the number of the C atoms in the structures of the metal complexes. The ESI-MS spectra of **1–6** exhibit essential mass peaks assignable to the $[M+Na]^+$ species suggesting that they retain their composition in solution and the presence of the peaks associated with the $[M–barb]^+$ moieties also indicates the dissociation of these complexes by losing a barb anion under the ESI-MS ionization conditions. In the case of complex **6**, the $[Pt(dpya)_2–H]^+$ and $[Ag(barb)_2+2Na]^+$ species are present in the solution.

Owing to their higher cytotoxicities, complexes **1**, **2** and **5** were selected for stability assay. The stability studies were performed in MeOH, used to prepare the stock solutions of the complexes, and the saline solution (0.9% NaCl), typically used for intravenous infusion of platinum complexes. The MeOH solutions were kept at room tempterature, while the saline solutions were incubated at 37°C. The stability of the complexes (1 mM) in both solutions was analyzed using reverse phase HPLC at 0 and 24-h intervals.[43,44] The initial amount (t = 0 h) of the complex is considered as 100% value and the stability of the complex after 24 h was expressed as the percentage of the remaining complex compared to the initial amount. Stabilities of **1**, **2** and **5** were estimated as 96, 95 and 93%, respectively, in MeOH and 94, 97 and 95%, respectively, in the saline solution (ESI Fig. S1†). From these results, it is evident that the present complexes in MeOH and the saline solutions showed high stabilities, maintaining the integrity of their molecular structures after 24 h.

Description of crystal structures

The structures of complexes **1** and **3–6** were determined by X-ray diffraction measurements. The summary of data collection, structure solution and refinement details are presented in Table 1. The MERCURY drawings including the atom numbering schemes of complexes **1** and **3–6** are shown in Fig. 1.

The crystal structure of **1** consists of discrete binuclear species, in which two palladium atoms are doubly bridged by two barb ligands with a μ_2-N/O bridging mode via the negatively charged N and one of the carbonyl O atoms (Fig. 1). The coordination of palladium(II) through the carbonyl O atom of barb was observed for the first time here and the N/O bridging behaviour of this ligand closely resembles those of the 1-methyluracil and 1-methylthymine ligands in their palladium(II) complexes.[45,46] The pyrimidine rings of two barb

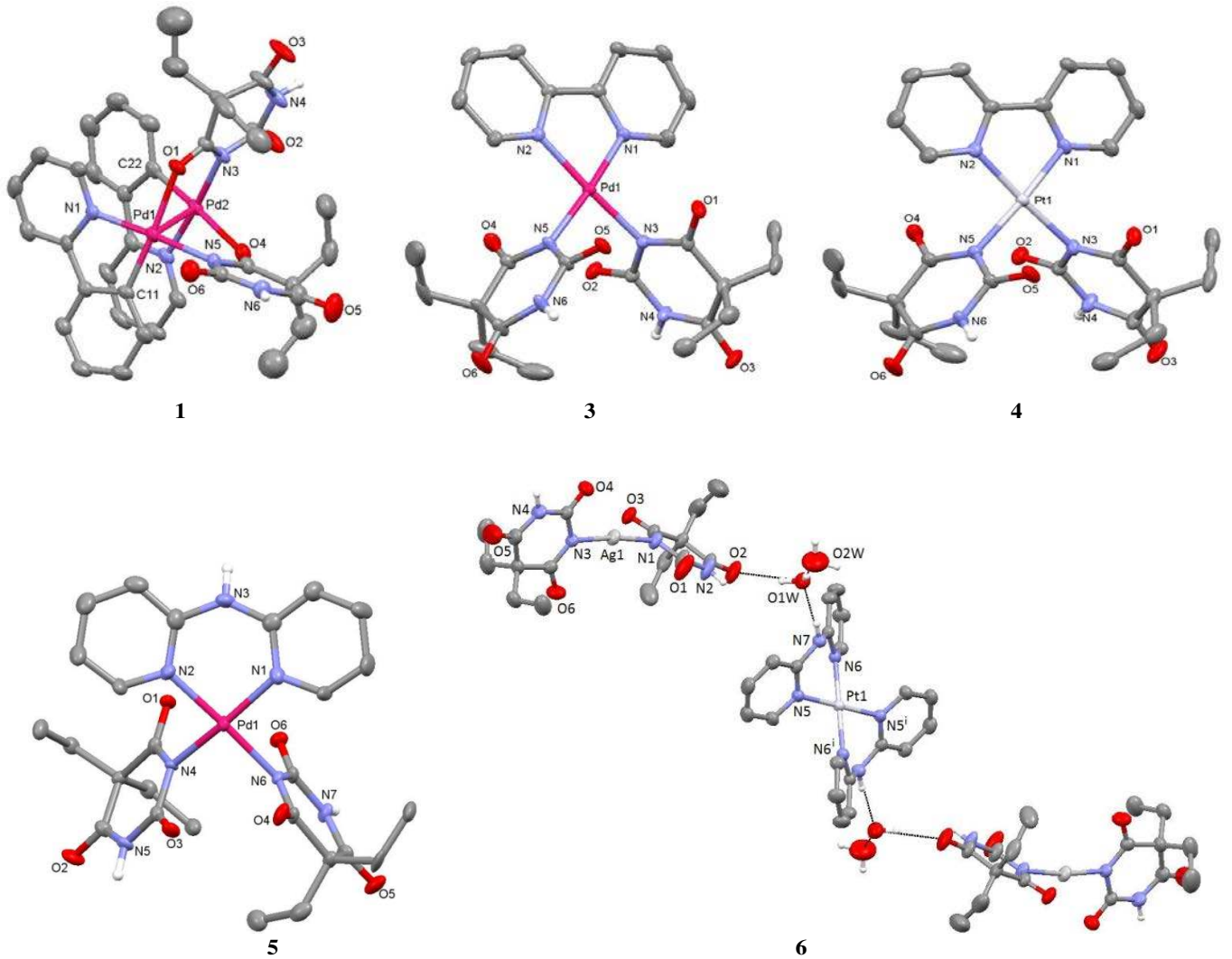

Fig. 1 The molecular structures of $[Pd_2(\mu\text{-barb})_2(ppy)_2]$ (**1**), $[Pd(barb)_2(bpy)]$ (**3**), $[Pt(barb)_2(bpy)]$ (**4**), $[Pd(barb)_2(dpya)]$ (**5**) and $[Pt(dpya)_2][Ag(barb)_2]_2{\cdot}4H_2O$ (**6**). Thermal ellipsoids are drawn at 50% probability for **1** and 40% probability for **3**–**6**. All CH hydrogen atoms are omitted for clarity. Selected bond lengths (Å) and angles (°) for **1**: Pd1–N1 2.022(5), Pd1–N5 2.071(5), Pd1–O1 2.179(4), Pd1–C11 1.958(6), Pd2–N2 2.024(5), Pd2–N3 2.067(5), Pd2–O4 2.162(5), Pd12–C22 1.962(7), Pd1–Pd2 2.8909(7), C11–Pd1–N1 81.2(3), C11–Pd1–N5 94.6(3), N1–Pd1–N5 174.4(2), C11–Pd1–O1 175.0(2), N1–Pd1–O1 93.91(19), N5–Pd1–O1 90.25(18), C22–Pd2–N2 81.3(3), C22–Pd2–N3 95.1(3), N2–Pd2–N3 176.0(2), C22–Pd2–O4 173.7(2), N2–Pd2–O4 93.4(2), N3–Pd2–O4 90.27(19); for **3**: Pd1–N1 2.018(3), Pd1–N2 2.026(3), Pd1–N3 2.039(3), Pd1–N5 2.041(3), N1–Pd1–N2 80.67(12), N1–Pd1–N3 94.96(12), N1–Pd1–N5 175.21(11), N2–Pd1–N3 175.45(11), N2–Pd1–N5 95.97(12), N3–Pd1–N5 88.32(12); for **4**: Pt1–N1 2.005(3), Pt1–N2 2.013(3), Pt1–N3 2.041(3), Pt1–N5 2.041(3), N1–Pt1–N2 80.38(14), N1–Pt1–N3 95.51(14), N1–Pt1–N5 175.89(12), N2–Pt1–N3 175.70(13), N2–Pt1–N5 96.48(14), N3–Pt1–N5 87.56(14); for **5**: Pd1–N1 2.040(7), Pd1–N2 2.048(6), Pd1–N4 2.051(5), Pd1–N5 2.067(5), N1–Pd–N2 89.1(3), N1–Pd1–N4 171.0(2), N1–Pd1–N6 93.7(2), N2–Pd1–N4 90.6(3), N2–Pd1–N6 177.1(2), N4–Pd1–N6 86.5(2); for **6**: Pt1–N5 2.0143(18), Pt1–N6 2.0155(19), Ag1–N1 2.114(2), Ag1–N3 2.109(2), N5–Pt1–N6 85.76(8), N5–Pt1–N6^{i} 94.24(8), N1–Ag1–N3 172.91(8). Symmetry code: $-x+1, -y+1, -z+1$.

ligands are perpendicular to the coordination plane in order to reduce steric hindrance, while the two ppy rings are oriented roughly parallel to each other with a dihedral angle of 10.5(2)°, giving rise to a weak π–π interaction of 3.767(5) Å. The bridging of two palladium centers results in a significantly short Pd–Pd distance of 2.8909(7) Å, which is similar to that of found in $[\{Pd(\mu\text{-sac})(ppy)\}_2]$ (sac = saccharinate)[38] and $[(bpy)Pd(l\text{-MeT})_2Pd(bpy)]^{2+}$ (l-MeT = l-methylthymine),[46] but it is much shorter than those reported for the palladium dimers.[47,48] The Pd–N(barb) distances compare well with those reported in the barb bridging palladium(II) complexes $(Et_4N)_6[\{Pd_3(Br_3L)\}_6(\mu\text{-barb})_9]$ and

$(Et_3NH)_4(Et_4N)_4[\{Pd_3(Br_3L)\}_4(\mu\text{-barb})_4(Hbarb)_4]$, containing μ_2-N/N bridging barb ligands.[32] The Pd–C and Pd–N distances, and N–Pd–C angles involving the cyclometalated ppy ligands are well within the range reported for palladium(II) complexes of ppy such as [Pd(py)(sac)(ppy)], $[\{Pd(\mu\text{-sac})(ppy)\}_2]$,[49] $[Pd(\mu\text{-}Cl_2)(ppy)_2]$[50] and $[Pd(ppy)\{P(X))Ph_2\}][PF_6]$.[51] The binuclear molecules of **1** are linked by N–H···O hydrogen bonds and π–π stacking interactions of 3.5846(2) Å, involving the ppy rings.

Complexes **3** and **4** are isostructural with a molecular formula of $[M(barb)_2(bpy)]$ (Fig. 1). The large distortions in the square-planar geometry of both complexes are originated from the bite angle of bpy [80.67(12)° for **3** and 80.38(14)° for **4**]. In addition, due to the presence of two alkyl groups, the barb ligands tend to be oriented to each other with dihedral angles of 73.2(2) and 72.9(2)° for **3** and **4**, respectively. Similar repulsive forces were observed between the methyl groups of two mesitylene (mes') ligands in $[(np)Pt(mes')_2]Cl_2$.[52] The M–N(bpy) bond distances are in the expected range for palladium(II) and platinum(II) complexes of this type.[46, 53-61] Both M–N(barb) bond distances are typical of those found in palladium(II) and platinum(II) complexes containing the monodentate barb ligand.[30-32] The molecules of **3** and **4** are linked by the N–H···O hydrogen bonds along the c axis to form hydrogen-bonded chains. Then, these chains are further connected via π–π interactions.

Complex **5** consists of individual molecules of $[Pd(barb)_2(dpya)]$, in which the dpya ligand coordinates to the palladium(II) ion via two pyridyl N atoms, while both barb ligands are N-bonded (Fig. 1). The dpya ligand is not planar and adopts a boat conformation and the dihedral angle between two py rings is 21.1(3)°. Again, the pyrimidine rings of the barb ligands are oriented with a dihedral angle of 73.8(2)°. The Pd–N(barb) distances are somewhat longer than those found in **3**, while the Pd–N(dpya) bond distances are close agreement with those found in palladium(II) complexes of the dpya ligand.[39,62,63] In the crystal, the molecules are triply bridged by the N–H···O hydrogen bonds, leading to layers propagating in the (000) plane.

As shown in Fig. 1, complex **6** is composed of a $[Pt(dpya)_2]^{2+}$ cation, two $[Ag(barb)_2]^-$ anions and four water molecules of crystallization. In the cation, the platinum(II) ion is located on the inversion centre and coordinated by two bidentate dpya ligands. The Pt–N(dpya) bond distances are similar to those reported for the platinum(II) complexes of dpya.[39,40,65-67] In the complex anion, the silver(I) ion is coordinated lineraly by two barb ligands. The Ag–N(barb) bond distances compare well with the corresponding bonds found in the silver(I) complexes containing linearly coordinated barb ligands.[33,34,68,69] In the crystal, the $[Ag(barb)_2]^-$ anions are linked by N–H···O hydrogen bonds into a chain and the $[Pt(dpya)_2]^{2+}$ cations are further connected to these chains, through symmetrically related water molecules, by OW–H···O hydrogen bonding interactions to form a three-dimensional supramolecular network.

Interaction with DNA

Electronic absorption titration. The UV-Vis spectra of complexes **1**–**6** in the absence and presence of FS-DNA exhibited a hyperchromic effect around ca. 245 nm (Table 2, Fig. 2, ESI Fig. S2†). The spectra of **1**, **2**, **5** and **6** displayed a 4 nm red-shift, while no shift was observed in those of **3** and **4**. In order to compare the DNA binding affinities, the intrinsic binding constant K_b was calculated using the equation:[70]

$$[DNA]/(\varepsilon_a-\varepsilon_f) = [DNA]/(\varepsilon_b-\varepsilon_f) + 1/K_b(\varepsilon_b-\varepsilon_f) \quad (1)$$

where [DNA] is the concentration of DNA in base pairs, ε_a, ε_f and ε_b correspond to $A_{obs}/[M]$, the extinction coefficient of the free metal complex and the extinction coefficient of the complex in the fully bound form, respectively. The ratio of slope to intercept in the plot of $[DNA]/(\varepsilon_a-\varepsilon_f)$ versus [DNA] gives the value of K_b. The K_b values in Table 2 range from 4.5 x 10^4 to 2.0 x 10^5 M^{-1}, suggesting a significant association of these complexes with FS-DNA. Complexes **1** and **2** showed higher K_b values, which are the same as that observed for the hyperchromism. However, their binding constants are similar to those of some platinum(II) complexes of bpy and terpy,[18,71] but they are lower than that reported for the classical intercalator, ethidium bromide (EB) (K_b = 1.4 x 10^6 M^{-1})[72] and the platinum(II) complexes with bpy and derivatives.[73]

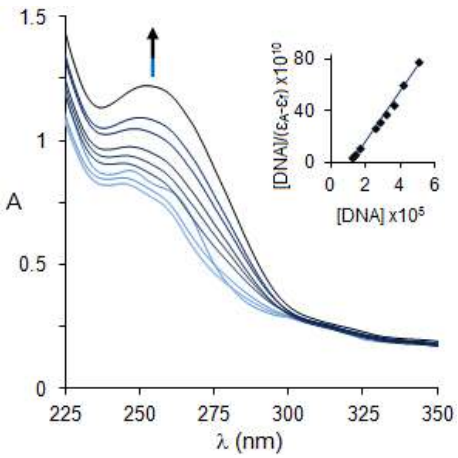

Fig. 2 Electronic absorption spectra of complexes **1** (25 μM) upon the titration of FS-DNA (0–50 μM) in Tris-HCl buffer. The arrow shows the increases in absorbance with respect to an increase in the FS-DNA concentration. The inset shows the linear fit of $[DNA]/(\varepsilon_a - \varepsilon_f)$ vs. [DNA] and the binding constant (K_b) was calculated using equation (1).

Ethidium bromide exchange. An appreciable decrease in emission intensity of EB bound FS-DNA was observed upon incremental addition of **1**–**6** (Fig. 3 and ESI Fig. S3†) and is indicative of an intercalative or minor groove binding.[74–78] The quenching ability of the complexes is evaluated by the Stern-Volmer quenching constant (K_{SV}):[79,80]

$$F_0/F = 1 + K_{SV}[Q] = 1 + k_q\tau_0[Q] \quad (2)$$

where F_0 and F are the fluorescence intensities in the absence

and presence of the complexes, respectively. [Q], k_q and τ_0 are the total concentration of the quencher (**1**–**6**), the quenching rate constant and the average lifetime of EB-DNA in the absence of the quencher ($\tau_0 = 10^{-8}$ s)[81], respectively. On the other hand, the apparent binding constant (K_{app}) is determined from the equation (3).[74]

$$K_{EB}[EB] = K_{app}[Q] \quad (3)$$

in which [Q] is the concentration of the quencher causing a 50% reduction in the fluorescence intensity of EB-bound DNA, $K_{EB} = 1.0 \times 10^7$ M^{-1} and [EB] = 5.0 μM.

The K_{SV} and K_{app} values in Table 2 suggest that **6** has a negligible effect on the fluorescence intensity of the EB-FS-DNA solutions, while the others bind significantly to DNA, suggesting intercalative or minor groove mode of binding. Among all complexes, **1** and **5** exhibit stronger binding propensity.

Since dynamic and static quenching processes are both temperature dependent The K_{SV} values estimated from the measurements performed at 293, 301 and 310 K were gradually decreased with the increasing of the temperature and clearly indicate a static quenching path.[81]

Hoechst 33258 displacement. The competitive DNA binding measurements with Hoechst 33258 showed that the addition of complexes **1** and **3** resulted in a significant decrease in the fluorescence intensity of the Hoechst-DNA solutions (Fig. 3 and ESI Fig. S4†). The quenching constant of **1** ($63.6 \pm 1.6 \times 10^4$ M^{-1}) is approximately 7-fold higher than that of **3** ($8.7 \pm 0.2 \times 10^4$ M^{-1}). However, the rest of the complexes have practically no influence on the intensity of the Hoechst-DNA system. Thus, complexes **1** and **3** displace the minor-groove fluorogen Hoechst 33258 with greater specificity than intercalated EtBr and may be considered as DNA minor groove binders.

Viscosity studies. The relative viscosity of the FS-DNA solutions increases steadily, to a small extent, with increasing concentrations of **1**–**6**. The corresponding data were presented in ESI Fig. S5† as $(\eta/\eta_0)^{1/3}$ versus the ratio of the concentration (r) of the complex-FS-DNA solutions, where η is the viscosity of DNA in the presence of complex, and η_0 is the viscosity of DNA alone in the buffer solution.[82] The higher viscosity values were observed for **2** and **5**. The results of the viscosity measurements indicate that the complexes bind to FS- DNA via threading intercalation, being partially intercalated to DNA as well as binding within the grooves of DNA.[83,84]

DNA melting studies. The dissociation of the double strands into single strands occurs as the temperature of DNA solutions increases and the temperature at which half of the total base pairs is unpaired is defined as the DNA melting

Table 2 Binding (K_b and K_{app}) and quenching constants (K_{SV}) for the interaction of **1**–**6** with FS-DNA

Complexes	UV titration		EB exchange	
	K_b (M^{-1}) x 10^{-4}	Δε (%)	K_{SV} (M^{-1}) x 10^{-4}	K_{app} (M^{-1}) x 10^{-6}
1	20.0 ± 2.4	35.6	4.7 ± 0.1	4.0
2	10.0 ± 0.8	25.4	3.2 ± 0.2	1.5
3	5.5 ± 0.1	10.4	2.4 ± 0.2	1.0
4	6.0 ± 0.1	19.5	1.4 ± 0.1	1.0
5	7.0 ± 0.4	31.2	4.9 ± 0.1	2.0
6	4.5 ± 0.1	23.8	0.5 ± 0.1	–

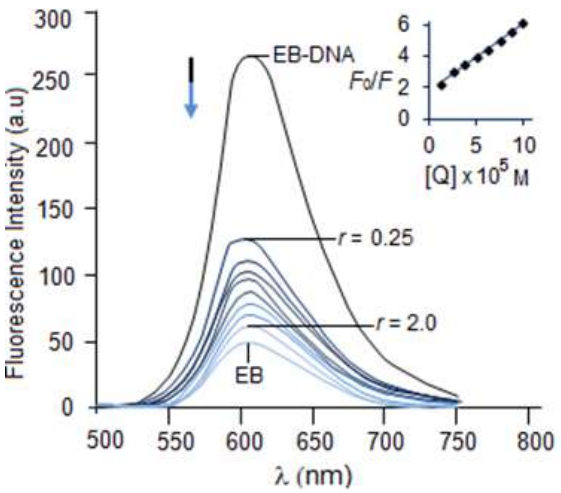

(**a**)

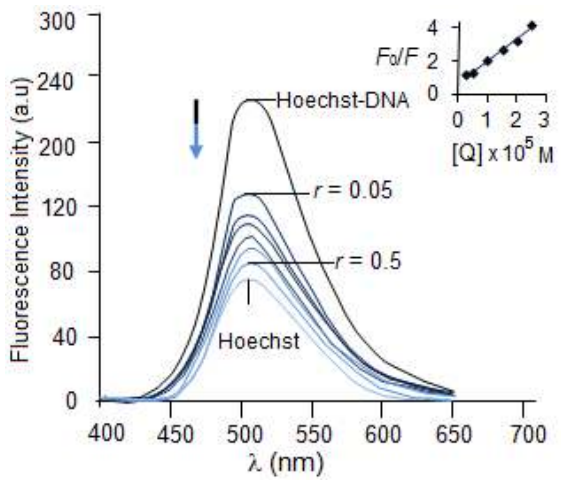

(**b**)

Fig. 3 Emission spectra of EB-bound (**a**) and Hoechst 33258-bound (**b**) DNA solutions in the absence and presence of increasing concentrations of complexes **1** (12.5–100 μM for **a** and 2.5–25 μM for **b** in Tris-HCl buffer. [EB] = [Hoechst 33258] = 5.0 μM, [DNA] 50.0 μM. r = [complex]/[DNA]. The arrows show the changes in intensity upon increasing amounts of the complexes. Insets: Stern-Volmer plot of the fluorescence data.

temperature (T_M).[85,86] Thermal melting on FS-DNA(ESI Fig. S6†) revealed that complexes **1**, **2, 5** and **6** extensively stabilized the thermal denaturation (ΔT_M = 6, 15, 11, 3 ºC, respectively), while the other complexes yielded either no or negligible effects under our tested conditions. In general, a high ΔT_M value corresponds to an intercalative mode of binding of a metal complex to DNA, while a low value indicates a non-intercalative binding mode.[87-89]

DNA Cleavage

Electrophoretic mobility. The chemical nuclease activity of complexes **1**–**6** towards the supercoiled plasmid pUC19 DNA was studied by agarose gel electrophoresis in the absence of any external effect such as UV light, reducing and oxidizing agents. The nuclease efficiency of the complexes was assessed by their ability to convert the closed circular supercoiled from of the DNA (form I) to the open circular relaxed form (form II) or the linear form (form III). All complexes were initially interacted with the plasmid DNA at the various [complex]/[DNA] ratios (*r*) of 0.5, 1.0, 2.0 and 5.0 in a relatively short incubation time (30 min) at 37 °C. It was shown that the plasmid DNA is not cleaved in the presence of complexes **5** and **6**, being very similar to the control, while the mobility of the form I band decreases with increasing amounts of **3** and **4**, indicating conformational changes (unwinding) in the plasmid DNA due to the non-covalent binding of these complexes (Fig. 4). In contrast, the lanes for **1** and **2** contained no bands corresponding to form I or any cleaved form II or form III; instead, a smearing of DNA occured giving a clean gel image without any DNA residue in the gel even at r = 0.2. When the two complexes were restudied at much lower *r* values between 0.05-0.2, the form I band became discernible as a faint band with smearing at r = 0.05 for **1** and 0.075 for **2** compared to control (Fig. 4). Again, no forms of II and III were detected. The DNA smears reveal that EB used to stain DNA in the gel is completely expelled out of the plasmid DNA due to strong intercalation or groove binding of these complexes, leading to quenching of the EB emission (see competitive binding studies). Similar behavior of the plasmid DNA in the gels stained with EB was reported previously for ruthenium(II) complexes bearing diimine ligands such as dpya[90] and phen.[91]

Inhibition of restriction enzymes. To investigate binding preference of complexes **1**–**6**, a restriction enzyme inhibition assay was used. Restriction enzyme inhibition by metal complexes is due to the fact that when a metal complex binds at the unique binding site of a restriction enzyme on DNA, it tends to inhibit the endonuclease activity of the enzyme by blocking its recognition site.[92-94] Consequently, a metal complex that inhibits a restriction enzyme is said to bind selectively.

In this study, two representative restriction enzymes, which differ in their target sequence, namely *Hin*dIII (recognition site AAT↓ATT) and *Bam*HI (recognition site G↓GATCC), were chosen. Both enzymes have single restriction site in pUC19 plasmid DNA and were tested to observe inhibition of their endonuclease activity by presence of the complexes (Fig. 5). The formation of the linear form of pUC19 (form III) is clearly

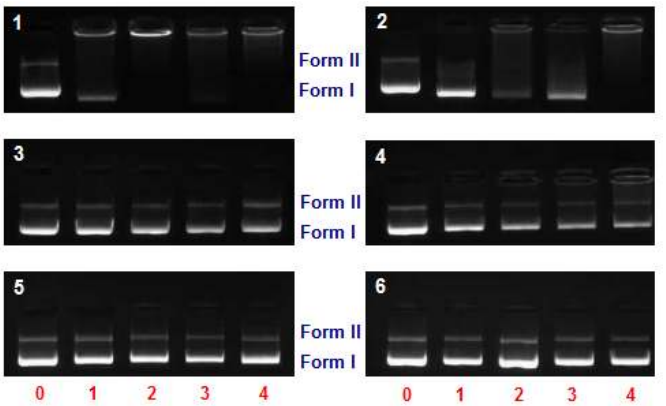

Fig. 4 Agarose gel electrophoresis images of pUC19 plasmid DNA incubated for 30 min at 37 °C with increasing concentrations of complexes **1**–**6**. Lane 0: pure plasmid DNA; lanes 1-4: DNA + complexes with r = 0.05, 0.075, 0.1 and 0.2, respectively, for complexes **1** and **2** and r = 0.5, 1.0, 2.0 and 5 for complexes **3**–**6**. Each sample contains 200 ng of plasmid DNA.

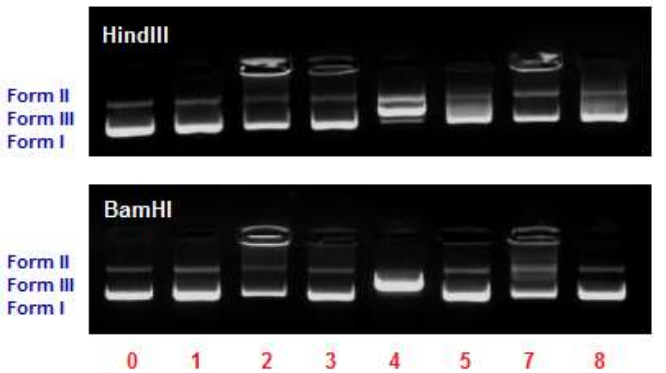

Fig. 5 Restriction endonuclease activity of complexes **1**–**6** towards pUC19 plasmid DNA. Agarose gel electrophoresis images showing formation of restriction digestion products of *Hin*dIII and *Bam*HI enzymes on pUC19 after incubation with complexes **1**–**6**. Lane 0: pure plasmid DNA; lane 1: enzyme + DNA; lanes 2-8: enzyme + DNA + complexes **1**–**6**, respectively. r = 0.05 for complexes **1** and **2**; r = 1.0 for complexes **3**–**6**.

visible only for complex **3** in both cases. The activity introduced in the plasmid by *Hin*dIII restriction endonuclease was found to be notable for complexes **1**–**6**, indicating their preference to the A/T binding. Moreover, complexes **1**, **3** and **5** have a tendency to bind with both G/C and A/T rich sequences.

Molecular docking

Molecular docking is a well-established computational technique for predicting the interaction between the molecules and DNA, and to find the binding and best orientation of the molecule, which would form a new complex with overall minimum energy. In this context, the Protein Data Bank was searched and two structures of B-DNA were selected: a dodecamer $d(CGCGATATCGCG)_2$ (1DNE) for groove binding and an octamer $d(GAAGCTTC)_2$ (1DSC) for intercalation.[95] Then, complexes **1**–**6** were docked into DNA to study the proper binding site along with preferred orientation of the complexes inside these DNA duplexes. The lowest-energy

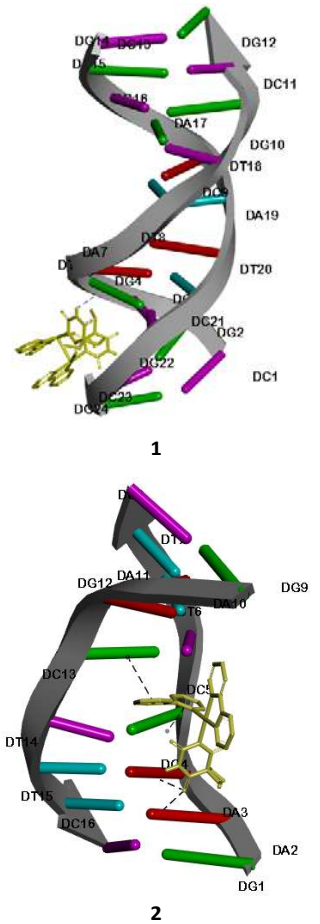

Fig. 6 Computational docking models (using the Autodock/Vina software) illustrating the interactions between DNA and complexes **1** and **2**.

conformations show that **1** and **3** bind to the minor groove near the domain of the G base (Fig. 6 and ESI Fig. S7†), while complexes **2**, **4**–**6** interacts with DNA with a partial intercalation together with hydrogen bonding interactions with the A rich regions in the grooves.

There are weak π–π stacking interactions between the aromatic rings in complexes **2**, **4**, **5** and DNA. Furthermore, all complexes favour the formation of hydrogen bonding mainly through the barb ligands, which act as hydrogen bond donor and acceptor due to the presence of the NH and carbonyl groups (Table S1). The $[Pt(dpya)_2]^{2+}$ cation in **6** is not involved in hydrogen bonding and interacts electrostatically with DNA, while the $[Ag(barb)_2]^-$ anion forms two hydrogen bonds with the A and C bases (ESI Fig. S7†). Overall, these interactions contribute significantly to the stabilization of each complex within the DNA duplex.

The DNA binding affinity of the complexes may be predicted from the binding free energy. The calculated binding free energies for **1**–**6** are in the range of 27.61-32.22 kJ mol^{-1} (Table S1) and follow the same order obtained for the binding constants of the complexes. Finally, the modes of binding of the complexes with DNA obtained from molecular docking studies correspond well with the experimental findings.

Table 3 Radical scavenging activities of complexes **1**–**6**

	IC50 (μM) ± esd	
Compounds	$DPPH^{\bullet}$	$ABTS^{\bullet+}$
1	52.3 ± 1.7	51.2 ± 3.4
2	39.7 ± 1.3	28.9 ± 2.3
3	99.7 ± 3.2	92.8 ± 1.4
4	136.2 ± 3.9	113.6 ± 2.7
5	117.8 ± 3.3	108.2 ± 3.1
6	121.4 ± 2.6	111.3 ± 4.2
Na(barb)	34.1 ± 1.9	30.2 ± 2.4
BHT	15.9 ± 1.2	11.4 ± 1.1
Ascorbic acid	11.3 ± 1.6	4.1 ± 0.9

Antioxidant properties

The presence of hydrogen donating ligands allows the suggestion that these complexes may display antioxidant properties. The antioxidant potentials of complexes **1**–**6** were tested by two models, namely 2,2-diphenyl-2-picryl-hydrazyl (DPPH) and 2,2'-azino-bis(3-ethylbenzthiazoline-6-sulfonic acid) (ABTS), and compared with well-known standards such as the natural antioxidant ascorbic acid and a synthetic antioxidant butylated hydroxytoluene (BHT). The DPPH radicals are stable in solution, being a useful reagent for the investigation of the radical scavenging activity of phenols, catecholes, thiols etc..[96] The radical activity of a compound can be monitored spectrophotometrically by measuring the decrease in the absorbance of DPPH at 517 nm as well as a colour change from violet to yellow. The ABTS test is usually used to evaluate the total antioxidant capacity of many compounds,[97] because the ABTS radical can react not only with the hydrogen donating compounds such as phenols, but also with any compound giving a hydrogen atom or an electron. The absorption of the $ABTS^{\bullet+}$ radical centred at ca. 740 nm (giving a bluish-green colour) diminishes rapidly in the presence of an antioxidant, yielding the solution decolourization.

The scavenging effects of the complexes and the standards on DPPH and ABTS radicals were expressed as IC_{50} values, which correspond to the 50% inhibitory concentration (Table 3). The antioxidant activity of the complexes increased with increase in the concentration of the complexes. In general, the DPPH and ABTS radical scavenging activity of the complexes was low in comparison to that of the standard compounds. Moreover, the complexes were more effective in inhibition of the ABTS radical than the DPPH radical. Complexes **1** and **2** present a moderate reducing ability of both radicals. The IC_{50} values demonstrate that in each case, complex **2** exhibits greater antioxidant activity than the other complexes. The barb ligand contains an acidic NH group and the antioxidant activityof Na(barb) is most likely due to the donation facility of the NH hydrogen to the DPPH and ABTS free radicals. The lower radical scavenging activity of the complexes compared to Na(barb) under the same experimental conditions suggests that the H donation ability of the barb ligand significantly decreases upon coordination. The observed antioxidant activity of the complexes may be due to reduction in the radical character of DPPH and ABTS by transfer of a hydrogen atom from the barb ligands, rather than an electron donation.

Table 4 In vitro cytotoxic activity of complexes **1–6** after 48 h incubation

Complexes	IC_{50} (μM) ± esd			
	HT-29	MCF-7	DU-145	PNT1A
1	37.3 ± 0.9	50.4 ± 5.3	26.6 ± 1.1	81.2 ± 1.1
2	62.9 ± 1.7	78.4 ± 1.6	39.4 ± 1.8	52.7 ± 0.9
3	164.5 ± 8.8	98.7 ± 5.4	193.6 ± 5.0	124.5 ± 1.0
4	>300	224.9 ± 16.4	>300	142.6 ± 1.5
5	28.7 ± 1.8	41.2 ± 2.5	34.1 ± 3.1	64.1 ± 2.9
6	>300	230.6 ± 8.1	>300	123.1 ± 7.9
Cisplatin	42.0 ± 5.2	30.7 ± 1.3	4.5 ± 0.4	12.3 ± 0.9
Carboplatin	>300	>300	85.8 ± 10.2	108.3 ± 12.4
Oxaliplatin	44.4 ± 2.4	19.6 ± 1.8	4.3 ± 1.1	17.9 ± 0.7

Cellular uptake

Cellular uptake experiments are essential for the evaluation of permeability and mechanisms of transport of metal compounds on the cellular level. Human prostate cancer cells (DU-145) were incubated with the selected complexes (**1**, **2** and **5**) (50 μM) at 37 °C for 1 h and the Pd and Pt contents in the different subcellular fractions (membrane, cytoskeleton, cytosol and nucleus) were determined by ICP-MS. Fig. 7 shows the distribution of the complexes between these fractions. The total cellular uptake of **2** (2.86 ng Pt/10^6 cells) is comparable to cisplatin (2.70 ng Pt/10^6 cells) in the same conditions, but higher than those of **1** (2.43 ng Pd/10^6 cells) and **5** (1.37 ng Pd/10^6 cells). In addition, it should also be noted that less than 2.7% of the applied complexes was taken up by the cells during their incubations. Complex **2** is almost uniformly distributed between the four cellular fractions and shows the highest nuclear uptake compared to the other complexes. However, **1** is accumulated mostly in the cytosol and membrane, while **5** is deposited in membrane and cytoskeleton fractions. The cellular uptake studies indicate that the complexes efficiently enter into DU-145 cells. The Pd and Pt levels of each complex differ in the subcellular fractions and the cellular uptake does not strongly correlate with the cytotoxicity of the present complexes. Similar observations were reported for platinum(II) complexes, when a constant dose is applied.[44,98]

In vitro cytotoxic activity

The encouraging results observed in DNA binding and DNA cleavage studies have directed us to investigate the cell growth inhibition of the title complexes. In vitro cytotoxic activities of complexes **1**−**6** against human carcinoma cell lines namely MCF-7 (breast), HT-29 (colon), DU-145 (prostate) and PNT-1A (human prostatic epithelial cell) were assessed by MTT assay. The concentrations of the complexes ranged from 3.125 μM to 300 μM. The cytotoxic activity of the complexes was shown to be dose-dependent. The IC_{50} values (50% inhibition of cell growth) of the complexes together with those of cisplatin, carboplatin and oxaliplatin after a 48 h treatment are given in Table 4. These values demonstrate that in general complexes **1**, **2** and **5** showed certain inhibitory effect on all cancer cell lines, while complexes **3**, **4** and **6** were found practically ineffective. Complexes **1**, **2** and **5** exhibited higher in vitro cytotoxicity than carboplatin in all cases, and also the activities of **1** and **5** against the HT-29 cells are greater than the three clinically used metallodrugs. In addition, these complexes had much lower toxicity on the prostatic epithelial cells (normal cells), confirming that they act selectively for the HT-29 cells. Further studies are warranted to assess their biological properties in vivo and elucidate their actual mechanisms. On the other hand, there are differences in the cytotoxic activity of the present metal complexes. For example, **5** is the most cytotoxic on both HT-29 and MCF-7 cells, while **1** is most potent against DU-145 cells. Morever, **2** exhibits an activity between them. Although the complexes interact with DNA strongly, they display only moderate activities against the cells. These findings indicate that the cytotoxicity of the complexes is not correlated with their DNA binding propensities.

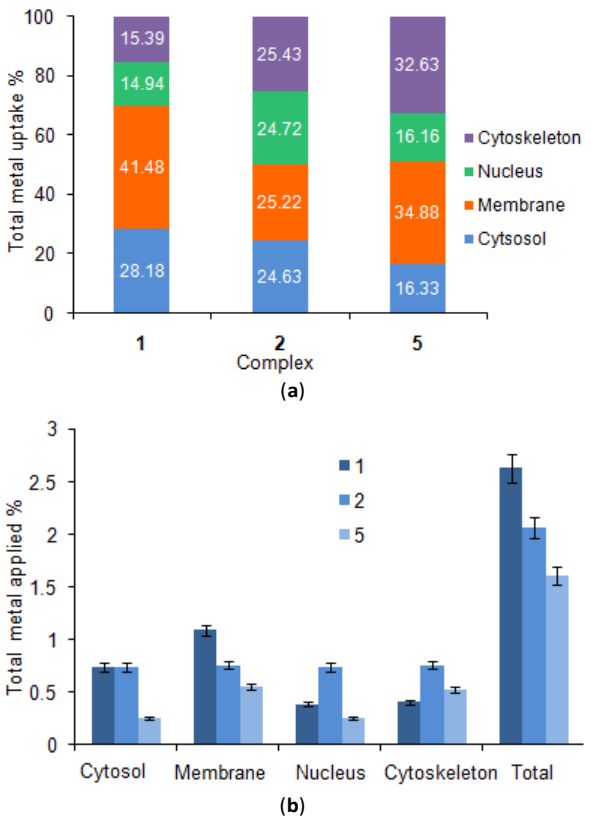

Fig. 7 Subcellular distribution of **1**, **2**, and **5** in DU-145 cells after 1 h of incubation at 37 °C with 50 μM concentration. (**a**) % of total uptake in the different fractions and (**b**) % of intracellular uptake of total amount applied.

Conclusions

Six new 5,5-diethylbarbiturato complexes of palladium(II) and platinum(II) with 2-phenylpyridine, 2,2'-bipyridine and 2,2'-dipyridylamine ligands were synthesized and characterized. The molecular structures of the complexes **1** and **3**–**6** were determined by single crystal X-ray diffraction, while that of **2** was deduced from elemental analysis, NMR and ESI-MS measurements. Complex **1** has a binuclear structure, while complexes **2**–**6** consist of mononuclear species. The UV-Vis, fluorescence spectroscopy, thermal denaturation and viscosity measurements revealed that the complexes bind strongly to FS-DNA. The binding constants of the complexes with DNA calculated for electronic absorption and fluorimetric competetive titrations showed that complexes **1**, **2** and **5** has higher binding affinity to DNA than the rest of the complexes. In addition, only **1** and **2** alters the DNA superhelicity upon binding with supercoiled pUC19 DNA, which is consistent with their higher DNA binding affinities. Based on the experimental data as well as DNA docking studies, the mode of binding was suggested as minor groove recognition for **1** and **3**, threading intercalation for **2** **4** and **5**, and a combination of electrostatic and groove binding for **6**. The cellular uptake studies suggest that in addition to DNA, these complexes might also interact with other cellular components. The antioxidant studies indicated that complexes **1** and **2** exhibited moderate activities compared to the reference antioxidants butylated hydroxytoluene and ascorbic acid. In addition, in vitro cytotoxic activities of the complexes against breast (MCF-7), colon (HT-29) and prostate (DU-145) cancer cell lines were assayed. Complexes **1** and **5** showed considerable cytotoxic activity specifically against HT-29 cells compared to clinically used metallodrugs such as cisplatin, carboplatin and oxaliplatin. However, the strong DNA binding ability of the complexes does not result in high cytotoxic activity against the cancer cells.

Experimental

Materials and measurements

All chemicals used in the experiments were purchased commercially and used without further purification. The starting complexes, $[MCl_2(L)]$ (M = Pd^{II} or Pt^{II}; L = bpy[37,38] or dpya[39,40]), were prepared as described in the literature. Tris(hydroxymethyl)aminomethane (Tris-HCl), ethidium bromide (EB), Hoechst 33258, 2,2-diphenyl-1-picrylhydrazyl (DPPH), 2,2'-azino-bis(3-ethylbenzthiazoline-6-sulfonic acid) (ABTS), L-ascorbic acid, butylated hydroxytoluene (BHT), plasmid DNA pUC19 and fish sperm (FS)-DNA, were obtained from Sigma, and loading buffer (10×) from was obtained from Dr. Zeydanli. The FractionPREP cell fractionation kit was purchased from Biovision. Doubly distilled water was used as the solvent throughout the experiments. The stock solution of FS-DNA was prepared in Tris-HCl buffer (20 mM Tris-HCl/20 mM NaCl buffer at pH 7.0). All stock solutions were stored at 5 °C and used within 3 days. The ratio of the UV absorbance at 260 and 280 nm (A_{260}/A_{280}) was checked to be ca. 1.86, indicating that the DNA is sufficiently free from protein contamination.[99] The DNA concentration per nucleotide phosphate [NP] was determined by the UV absorbance at 260 nm after 1:20 dilutions using the known ε value of 6600 $M^{-1}cm^{-1}$.[100]

Elemental analyses for C, H, and N were performed using a Costech elemental analyser. UV-Vis spectra were measured on a Perkin Elmer Lambda 35 spectrophotometer. IR spectra were recorded on a Perkin Elmer Spectrum Two FT-IR spectrophotometer. ^{1}H NMR and ^{13}C NMR spectra were recorded on a Varian Mercuryplus spectrometer at 400 and 100 MHz, respectively, in DMSO-d_6 using Me_4Si as internal reference at room temperature. Fluorescence spectra were recorded at room temperature with a Varian Cary Eclipse spectrophotometer equipped with a Xe pulse lamp of 75 kW. For all fluorescence measurements, the slits were maintained at 5 nm. The ESI mass spectra were recorded using a Bruker Daltonics Microtof II-ESI-TOF mass spectrometer. The electrical conductivity measurements of the complexes in MeOH and DMSO were carried out with Inolab Cond 730 conductimeter at room temperature and reported as Λ_M (S cm^2 mol^{-1}). Melting points are measured using a BUCHI 560 instrument and a capillary apparatus. The agarose gel electrophoresis was performed using UVITEC imaging and gel documentation systems.

Synthesis of palladium(II) and platinum(II) complexes

Synthesis of $[Pd_2(\mu\text{-barb-}\kappa N,O)_2(ppy\text{-}\kappa N,C)_2]$ (1). 71 µL (0.5 mmol) of 2-phenylpyridine (Hppy) was added to the solution of $PdCl_2$ (0.09 g, 0.5 mmol) dissolved in 25 mL of MeCN and this solution was refluxed at 60 °C for 3 h. Then, 10 mL aqueous solution of Na(barb) (0.154 g, 0.75 mmol) was added to this solution and stirred at 60 °C for 1 h. The yellow precipitate was filtered off and recrystallized from a mixture of MeCN, DMSO and isopropyl alcohol (1:1:1) (yield: 0.536 g, 76%; mp (decomp.) 330–334 °C). Anal. calc. for $C_{38}H_{38}N_6O_6Pd_2$ (%): C, 51.42; H, 4.32; N, 9.47. Found: C, 51.21; H, 4.65; N, 9.69. IR (KBr, ν/cm^{-1}) 3189m (NH-barb), 3067w (arom. CH), 2968w (aliph. CH), 2934w (aliph. CH), 1727m (CO), 1703s (CO), 1678vs (CO), 1606vs (CN), 1577s (CC), 1488m, 1403s, 1313vs, 1256vs, 1167w, 1019m, 950w, 828m, 737vs, 720vs, 548vs, 469m. ^{1}H NMR (400 MHz; DMSO-d_6; Me_4Si): δ (ppm) 10.74 (s, 2H, NH-barb), 9.25 (broad s, 2H, H^6-ppy), 8.46 (broad s, 2H, H^4-ppy), 8.04 (broad s, 6H, H^3, H^5, $H^{6'}$-ppy), 7.74-7.57 (t, ^3J(HH) = 6.8 Hz, 2H, $H^{5'}$-ppy), 7.40 (broad s, 4H, $H^{6'}$, $H^{4'}$-ppy), 7.14-6.95 (t, ^3J(HH) = 7.7 Hz, 2H, $H^{3'}$-ppy), 1.82-1.76 (q, 8H, ^3J(HH) = 7.6 Hz, CH_2-barb), 0.73-0.69 (t, 12H, ^3J(HH) = 7.6 Hz, CH_3-barb). ^{13}C NMR (100 MHz, DMSO-d_6; Me_4Si): δ 173.5, 165.8, 163.7 CO barb, 151.0 C2-ppy, 148.3 C6-ppy, 141.3 C1'-ppy, 136.7 C4-ppy, 132.9 C4'-ppy, 130.0 C5'-ppy, 129.0 C3'-ppy, 126.6 C2'-ppy, 125.1 C3-ppy, 120.0 C5-ppy 56.9 CEt_2-barb, 31.6 CH_2-barb, 9.6 CH_3-barb. UV λ_{max} (MeOH)/nm 304, 314 and 325 (ε/dm^3 mol^{-1} cm^{-1} 15200, 14400 and 10000). Molar conductivity, Λ_M (1×10^{-3} M, MeOH) 15 S cm^2 mol^{-1}

(nonelectrolyte) and Λ_M (1×10^{-3} M, DMSO) 6 S cm^2 mol^{-1} (nonelectrolyte). ESI-MS (*m/z*, MeOH): 910.2 $[M+Na]^+$ (calc.: 910.6), 852.8 $[Pd_2(ppy)_2(\mu\text{-}ppy)_2+Na]^+$ (calc.: 852.6).

Synthesis of [Pt(barb)(Hppy-κN)(ppy-κN,C)]·3H$_2$O (2). 71 μL (0.5 mmol) of Hppy was added to the solution of $K_2[PtCl_4]$ (0.21 g, 0.5 mmol) dissolved in 10 mL of water and this solution was refluxed at 60 °C for 1 h. Then, 10 mL aqueous solution of Na(barb) (0.154 g, 0.75 mmol) was added to this solution and stirred at 60 °C for 1 h. The yellow precipitate was filtered off and air-dried (yield: 0.526 g, 71%, mp 180–184 °C). Anal. calc. for $C_{30}H_{34}N_4O_6Pt$ (%): C, 48.58; H, 4.62; N, 7.55. Found: C, 48.43; H, 4.65; N, 7.69. IR (KBr, ν/cm^{-1}) 3498b (OH), 3176w (NH-barb), 3066m (arom. CH), 2969m (aliph. CH), 2938w (aliph. CH), 1714m (CO), 1681s (CO), 1607s (CN), 1559w, 1473s (CC), 1424m, 1362m, 1316s, 1244m, 1161m, 1072w, 1014w, 998w, 760s, 741vs, 696vs, 553m. ^{1}H NMR (400 MHz, DMSO-d_6; Me_4Si): δ (ppm) 10.46 (s, 1H, NH-barb), 8.56 (s, 2H, H^6, H^{6*}-ppy), 8.05-7.91 (d, ^3J(HH) = 8.4 Hz, 3H, H$^{2'*}$, H$^{6'}$, H^4-ppy), 7.85-7.76 (t, ^3J(HH) = 7.6 Hz, 2H, H^{3*}, H^3-ppy), 7.73-7.68 (td, ^3J(HH) = 7.2 Hz, 3H, H^{4*}, H^{5*}, H^5-ppy), 7.49-7.38 (dd, ^3J(HH) = 7.2 Hz, 2H, H$^{3'}$, H$^{4'}$-ppy), 7.25-7.22 (d, ^3J(HH) = 6.8 Hz, 2H, H$^{5'*}$, H$^{6'*}$-ppy), 6.84-6.80 (t, ^3J(HH) = 5.6 Hz, 3H, H$^{5'}$, H$^{4'*}$, H$^{3'*}$-ppy), 1.72-1.69 (q, 4H, ^3J(HH) = 7.2 Hz, CH_2-barb), 0.65-0.61 (t, 6H, ^3J(HH) = 7.2 Hz, CH_3-barb). ^{13}C NMR (100 MHz, DMSO-d_6; Me_4Si): δ 173.5, 162.7 CO barb, 159.6 C2*-ppy, 154.3 C2-ppy, 153.5 C6-ppy, 151.4 C6*-ppy, 150.2 C1'*-ppy, 149.8 C2'*-ppy, 139.2 C1'-ppy, 138.7 C4*-ppy, 137.1 C4-ppy, 132.5 C4'*-ppy, 131.2 C3'-ppy, 129.8 C2'-ppy, 129.2 C3'-ppy, 127.6 C4'-ppy, 126.9 C5-ppy, 126.5 C6'*-ppy, 124.6 C5'*-ppy, 123.5 C5*-ppy, 121.3 C3*-ppy, 56.9 CEt_2-barb, 31.7 CH_2-barb, 9.6 CH_3-barb. UV λ_{max} (MeOH)/nm 277, 307 and 328 (ε/dm^3 mol^{-1} cm^{-1} 20800, 8400 and 6000). Molar conductivity, Λ_M (1×10^{-3} M, MeOH) 11 S cm^2 mol^{-1} (nonelectrolyte) and Λ_M (1×10^{-3} M, DMSO) 6 S cm^2 mol^{-1} (nonelectrolyte). ESI-MS (m/z, MeOH): 710.2, $[M+Na]^+$ (calc.: 710.7), 504.5 $[Pt(ppy\text{-}\kappa N,C)_2+H]^+$ (calc.: 504.1).

Synthesis of [Pd(barb-κN)$_2$(bpy-κN,N')] (3). The solid $AgNO_3$ (1 mmol, 0.17 g) was added to a suspension of $[PdCl_2(bpy)]$ (0.5 mmol) in water (200 mL) and then, this suspension was refluxed for 6 h. After cooling to room temperature, the precipitate of AgCl was removed by filtering through Celite paste to obtain a clear yellow solution. The filtrate was concentrated to ca. 25 mL and followed by the addition of Na(barb) (1 mmol, 0.21 g) and stirred at 60 °C for 1 h. As soon as the addition of Na(barb), a yellow precipitate was formed. The final suspension was cooled to the room temperature and filtered off to separate the yellow solid. The powders were recrystallized from to yield their DMSO solvate crystals of $[Pd(barb)_2(bpy)]$ (yield: 0.773 g, 86%, mp (decomp.) 368–372 °C). Anal. calc. for $C_{26}H_{34}N_6O_8Pd$ (%): C, 46.96; H, 5.15; N, 12.64. Found: C, 47.20; H, 4.84; N, 12.44. IR (KBr, ν/cm^{-1}) 3175w (NH-barb), 3084w (arom. CH), 3044w (arom. CH), 2938w (aliph. CH), 2854w (aliph. CH), 1716m (CO), 1687s (CO), 1633vs (CO), 1601m (CN), 1499w, 1449m (CC), 1366s, 1323vs, 1247m, 1160w, 1039w, 949w, 771m, 545w. ^{1}H NMR (400 MHz, DMSO-d_6; Me_4Si): δ (ppm) 10.76 (s, 2H, NH-barb), 8.96-8.46 (d, 2H, ^3J(HH) = 7.2 Hz, H^6, H$^{6'}$-bpy), 8.31 (s, 2H, H^3, H$^{3'}$-bpy), 7.92 (s, 2H, H^4, H$^{4'}$-bpy), 7.69 (s, 2H, H^5, H$^{5'}$-bpy), 2.21-1.44 (m, 8H, ^3J(HH) = 7.6 Hz, CH_2-barb), 1.06-0.31 (d, 12H, ^3J(HH) = 7.6 Hz, CH_3-barb). ^{13}C NMR (100 MHz, DMSO-d_6; Me_4Si): δ 178.5, 175.2, 156.7 CO barb, 155.5 C2-bpy, 151.2 C6-bpy, 141.8 C4-bpy, 127.7 C3-bpy, 124.4 C5-bpy, 56.4 CEt_2-barb, 32.1 CH_2-barb, 10.2 CH_3-barb. UV λ_{max} (MeOH)/nm 239, 308 and 315 (ε/dm^3 mol^{-1} cm^{-1} 30000, 15600 and 14400). Molar conductivity, Λ_M (1×10^{-3} M, MeOH) 12 S cm^2 mol^{-1} (nonelectrolyte) and Λ_M (1×10^{-3} M, DMSO) 7 S cm^2 mol^{-1} (nonelectrolyte). ESI-MS (*m/z*, MeOH): 651.1, $[M+Na]^+$ (calc.: 651.9), 445.1 $[M–barb]^+$ (calc.: 445.7).

Synthesis of [Pt(barb-κN)$_2$(bpy-κN,N')] (4). The procedure and quantities of the reactants for the preparation of **4** were the same as for **3** with $[PtCl_2(bpy)]$ replacing $[PdCl_2(bpy)]$. Yellow prisms of **4** were formed by slow evaporation of the DMSO solution (yield: 0.611 g, 72%, mp (decomp.) 372–375 °C). Anal. calc. for $C_{26}H_{36}N_6O_9Pt$ (%): C, 40.47; H, 4.70; N, 10.89. Found: C, 40.77; H, 5.95; N, 11.03. IR (KBr, ν/cm^{-1}) 3179w (NH-barb), 3085w (arom. CH), 3045w (arom. CH), 2971m (aliph. CH), 2936w (aliph. CH), 2877w (aliph. CH), 1716m (CO), 1688s (CO), 1641vs (CO), 1607s (CN), 1452m (CC), 1400s, 1363vs, 1322vs, 1242m, 1028m, 953w, 1162w, 770m, 546w. ^{1}H NMR (400 MHz, DMSO-d_6; Me_4Si): δ (ppm) 10.82 (s, 2H, NH-barb), 8.72-8.55 (m, 2H, ^3J(HH) = 8.0 Hz, H^6, H$^{6'}$-bpy), 8.53-8.51 (d, 2H, ^3J(HH) = 7.6 Hz, H^3, H$^{3'}$-bpy), 8.51-8.47 (m, 2H, ^3J(HH) = 7.2 Hz, H^4, H$^{4'}$-bpy), 7.90-7.76 (m, 2H, ^3J(HH) = 7.2 Hz, H^5, H$^{5'}$-bpy), 1.75-1.63 (q, ^3J(HH) = 7.2 Hz, 8H, CH_2-barb), 0.75-0.47 (tt, ^3J(HH) = 7.2 Hz, 12H, CH_3-barb). ^{13}C NMR (100 MHz, DMSO-d_6; Me_4Si): δ 178.2, 174.5, 156.2 CO barb, 155.1 C2-bpy, 149.6 C6-bpy, 141.8 C4-bpy, 127.8 C3-bpy, 124.5 C5-bpy, 56.2 CEt_2-barb, 32.1 CH_2-barb, 10.0 CH_3-barb. UV λ_{max} (MeOH)/nm 247, 308 and 321 (ε/dm^3 mol^{-1} cm^{-1} 26000, 9600 and 12000). Molar conductivity, Molar conductivity, Λ_M (1×10^{-3} M, MeOH) 14 S cm^2 mol^{-1} (nonelectrolyte) and Λ_M (1×10^{-3} M, DMSO) 3 S cm^2 mol^{-1} (nonelectrolyte). ESI-MS (*m/z*, MeOH): 740.2, $[M+Na]^+$ (calc. 740.6), 534.1 $[M–barb]^+$ (calc. 534.5).

Synthesis of [Pd(barb-κN)$_2$(dpya-κN,N')] (5). The preparation method for **5** was the same as described for **3**, using dpya instead of bpy. Yellow crystals were collected by filtration (yield: 0.585 g, 91%, mp (decomp.) 292–296 °C). Anal. calc. for $C_{26}H_{31}N_7O_6Pd$ (%): C, 48.91; H, 4.90; N, 15.21. Found: C, 48.64; H, 4.85; N, 15.07. IR (KBr, ν/cm^{-1}) 3306w (NH-dpya), 3205m (NH-barb), 3145w (arom. CH), 3086w (arom. CH), 2963w (aliph. CH), 2936w (aliph. CH), 2878(w), 1720m (CO), 1674s (CO), 1637vs (CO), 1589m (CN), 1517w, 1483s (CC), 1436m, 1407s, 1363m, 1316s, 1242m, 1163w, 1038w, 958w, 772m, 541w. ^{1}H NMR (400 MHz, DMSO-d_6; Me_4Si): δ (ppm) 10.63 (s, 2H, NH-barb), 9.65 (s, H, NH-dpya), 8.18-7.96 (dd, 2H, ^3J(HH) = 7.2 Hz, H^6, H$^{6'}$-dpya), 7.90-7.69 (td, 2H, ^3J(HH) = 8.4 Hz, H^4, H$^{4'}$-dpya), 7.64-7.26 (m, 2H, ^3J(HH) = 8.4 Hz, H^3, H$^{3'}$-dpya), 7.03-6.81 (tt, 2H, ^3J(HH) = 7.2 Hz, H^5, H$^{5'}$-dpya), 1.78-1.50 (m, ^3J(HH) = 7.2 Hz, 8H, CH_2-barb), 0.72-0.47 (tt, ^3J(HH) = 7.6 Hz, 12H, CH_3-barb). ^{13}C NMR (100 MHz,

DMSO-d_6; Me_4Si): δ 177.7, 174.7, 154.6 CO barb, 154.3 C2-dpya, 147.3 C6-dpya, 137.4 C4-dpya, 115.7 C5-dpya, 111.6 C3-dpya, 55.8 CEt_2-barb, 31.8 CH_2-barb, 9.1 CH_3-barb. UV λ_{max} (MeOH)/nm 302 and 317 (ε/dm^3 mol^{-1} cm^{-1} 17200 and 14000). Molar conductivity, Λ_M (1×10^{-3} M, MeOH) 21 S cm^2 mol^{-1} (nonelectrolyte) and Λ_M (1×10^{-3} M, DMSO) 12 S cm^2 mol^{-1} (nonelectrolyte). ESI-MS (*m*/*z*, MeOH): 666.1, $[M+Na]^+$ (calc.: 666.9), 460.1 $[M–barb]^+$ (calc.: 460.8).

Synthesis of [Pt(dpya-κN,N')$_2$][Ag(barb-κN)$_2$]$_2$·4H$_2$O (6). The procedure for the preparation of **6** were the same as for **4** with dpya replacing bpy. The resulting yellow solid was recrystallized from a mixture of MeOH, MeCN and water (1:1:1) (yield: 0.945 g, 85%, mp (decomp.) 315–318 °C). Anal. calc. for $C_{54}H_{76}Ag_2N_{14}O_{16}Pt$ (%): C, 40.41; H, 4.60; N, 12.51. Found: C, 40.18; H, 4.55; N, 12.57. IR (KBr, ν/cm^{-1}) 3457bs (OH), 3416bs (OH), 3318w (NH-dpya), 3184m (NH-barb), 3065w (arom. CH), 2971m (arom. CH), 2934w (aliph. CH), 2872w (aliph. CH), 1693m (CO), 1665s (CO), 1642s (CO), 1567m (CN), 1534s, 1480vs (CC), 1439vs, 1363m, 1314s, 1267m, 1238m, 1164w, 1029w, 845w, 777m, 543w. ^{1}H NMR (400 MHz, DMSO-d_6; Me_4Si): δ (ppm) 10.63 (s, 4H, NH-barb), 9.65 (s, 2H, NH-dpya), 8.19-7.94 (dd, 4H, ^3J(HH) = 7.2 Hz, H^6, H$^{6'}$-dpya), 7.86-7.69 (td, 4H, ^3J(HH) = 8.4 Hz, H^4, H$^{4'}$-dpya), 7.64-7.25 (tt, 4H, ^3J(HH) = 8.4 Hz, H^3, H$^{3'}$-dpya), 7.01-6.81 (tt, 4H, ^3J(HH) = 7.2 Hz, H^5, H$^{5'}$-dpya), 1.79-1.47 (m, ^3J(HH) = 7.2 Hz, 16H, CH_2-barb), 0.72-0.50 (tt, ^3J(HH) = 7.6 Hz, 24H, CH_3-barb). ^{13}C NMR (100 MHz, DMSO-d_6; Me_4Si): δ 178.9, 154.5, 154.2 CO barb, 149.7 C2-dpya, 147.3 C6-dpya, 137.4 C4-dpya, 115.7 C5-dpya, 111.6 C3-dpya, 57.3 CEt_2-barb, 31.8 CH_2-barb, 9.1 CH_3-barb. UV λ_{max} (MeOH)/nm 251 (ε/dm^3 mol^{-1} cm^{-1} 13600). Molar conductivity, Λ_M (1×10^{-3} M, MeOH) 171 S cm^2 mol^{-1} (1:2 electrolyte) and Λ_M (1×10^{-3} M, DMSO) 74 S cm^2 mol^{-1} (1:2 electrolyte). ESI-MS (*m*/*z*, MeOH): 536.1, $[Pt(dpya)_2–H]^+$ (calc. 536.4), 520.1 $[Ag(barb)_2+2Na]^+$ (calc. 520.3).

Stability assays

The stability of the complexes was performed in MeOH and a saline solution (0.9% NaCl). 1 mL of 1 mM test compounds in MeOH and the saline solution (stock solution 10 mM in MeOH) was incubated at room temperature and 37°C, respectively. An Agilent 1200 HPLC system was used for determination of the complexes at 0 and 24-h intervals. Chromatographic separations were carried out using an XBridge C18 (4.6 x 250mm, 3.5 mm) column from Waters. The mobile phase consists of water (solvent A) and acetonitrile (solvent B). Gradient conditions are as follows: 0-8 min 30% B, 8-19 min 70% B, 16-19 min 90% B, 18-20 min 30% B, and the total run time is 20 min. Flow rate was 0.75 mL/min and injection volume was 20 µL. Data acquisition and preprocessing was done with Chemstation for LC (Agilent). The disappearance of the complexes over time was monitored at 254 nm and expressed as remaining percentage compared to the initial amount.

X-ray crystallography

The intensity data for **1** and **6** were collected with a STOE IPDS 2 diffractometer, while those for **3–5** were obtained using a Nonius KappaCCD diffractometer using Mo K_α radiation (0.71073 Å) in each case. The structures were solved by direct methods and refined against $|F|^2$ with the SHELX-97 program.[101] Compounds **1**, and **3–5** contain highly disordered DMSO molecules, which were eliminated from the refinement of these structures by means of the SQUEEZE subroutine of PLATON[102] and the hkl intensities were modified accordingly. All non-hydrogen atoms were found from the difference Fourier map and refined anisotropically, while all hydrogen atoms were placed and refined using a riding model. CCDC 1034029 (**1**), 1034030 (**3**), 1034031(**4**), 1034032 (**5**) and 1034033 (**6**) contain the supplementary crystallographic data for this paper. These data can be obtained free of charge via www.ccdc.cam.ac.uk/data_request/cif (or from the Cambridge Crystallographic Data Centre, 12 Union Road, Cambridge CB2 1EZ, UK; fax: (+44)1223-336-033; or deposit@ccdc.cam.uk).

DNA binding experiments

Stock solutions of metal complexes were prepared using MeOH and then diluting them suitably with Tris-HCl buffer to the required concentrations for all the experiments. Absorption spectral titration experiments were performed by maintaining a constant concentration of the complex (25 µM) and varying the FS-DNA concentration (0-50 µM). The UV-Vis spectra of the FS-DNA solutions in the presence of each complex was scanned against the Tris-HCl buffer solution in the wavelength range from 200 to 500 nm.

In the ethidium bromide (EB) fluorescence quenching experiments, DNA was pretreated with EB in the ratio [NP/EB] = 10 in Tris-HCl buffer and then, the complexes ranging from 12.5 to 100 µM were added to this solution. All solutions were allowed to equilibrate thermally at 20 ºC for about 30 min before measurements. The fluorescence spectra of the solutions were recorded in the range of 500-750 nm at λ_{ex} = 295 nm.

Competitive binding between Hoechst 33258 and the complexes was studied by measuring fluorescence intensity of Hoechst 33258-DNA solutions in the ratio [NP/Hoechst 33258] = 10 in the absence and presence of the compounds (12.5-100 µM) in Tris-HCl buffer. The fluorescence spectra of these solutions were recorded in the range of 400-650 nm at λ_{ex} = 351 nm.

For viscosity measurements, an Ubbelodhe viscometer was immersed in a thermostatic water-bath at 20.0 ºC. The concentration of FS-DNA in Tris-HCl buffer was 25 µM and the viscosity of the FS-DNA solutions were measured in the presence of increasing amounts of the complexes (12.5-50 µM). Flow time was measured with a digital stopwatch and each sample was measured three times, then an average flow time was calculated. Viscosity values were calculated from the observed flow time of DNA-containing solutions (t) corrected for the flow time of buffer alone (t_0), $\eta = t - t_0$.

Thermal denaturation measurements were performed with a Perkin-Elmer Lambda 35 UV/Vis spectrophotometer equipped with a Peltier temperature-controlled sample cell. The temperature of FS-DNA (100 μM) in the absence and presence of the complexes (50 μM) were carried out by monitoring the absorbance at 260 nm in the temperature range of 25–95 °C with a heating rate of 2.5 °C min^{-1} in Tris-HCl buffer. The melting temperature (T_m) values were determined graphically from the plot of relative absorbance (A/A_{25}) versus temperature, where A is the observed absorbance and A_{25} is the absorbance at 25 ºC.

Cellular uptake studies

To investigate cellular uptake and intracellular distribution of complexes **1**, **2** and **5**, DU-145 cells were exposed to 50 μM of each complex at 37 ˚C for 1 h. Treatments were stopped by removing the incubation medium and adding cold PBS. Then, cells were washed with cold phosphate-buffered saline (PBS) twice, tyripsinized, resuspended in medium (1:5 v/v) and counted using a hemocytometer. Different fractions of cells (cytosol, nucleus, membrane/particulate and cytoskeletal fractions) were isolated from these cell suspensions using FractionPREP cell fractionation kit (Biovision) according to the provided protocol. The fractions were digested with 65% HNO_3 (3 mL) at 70 °C for 3 h and then diluted with ultra pure water to a final volume of 5 mL. The Pd and Pt contents in the different fractions were measured using Agilent 7500 Series ICP-MS system with ^{114}In and ^{209}Bi used as internal standards. The metal contents obtained in ppb units were then expressed as ng/10^6 cells.

DNA cleavage experiments

Gel electrophoresis. The cleavage of pUC19 plasmid DNA by complexes **1–6** was monitored using agarose gel electrophoresis at room temperature. The gel electrophoresis experiments were performed by incubation of the samples containing 10 μM plasmid DNA and metal complex (0.5-50 μM) in 50 mM Tris-HCl/18 mM NaCl buffer (pH 7.2) at 37 ºC for 24 h. A dye solution (bromophenol blue 0.05%, sucrose 40%, 0,5% sodium lauryl sulfate (SDS) and 0.1 M EDTA) was added to the reaction mixture and then, the samples were electrophoresed for 1 h at 90 V on 1% agarose gel using 0.5X TBE buffer (pH 8.0). The gel was then stained using 1 μg cm^{-3} EB and photographed under UV light.

Restriction enzyme inhibition. The restriction enzyme inhibition assay was carried out to know the sequence-specific binding and evaluation of enzyme inhibition by complexes. pUC19 (10 μM) plasmid was incubated with 1 or 10 μM concentration of each of the complexes in DMSO at 37 ºC in 50 mM Tris–HCl/18 mM NaCl buffer (pH 7.2) for 24 h for complexes **3–6** and 30 min for complexes **1** and **2**. Then these solutions were incubated separately with HindIII and BamHI (2 units) for 1 h under similar conditions. The results of incubation were obtained from 1.5 % (w/v) agarose gel electrophoresis in 1x TAE buffer. The gel was then stained using 1 μg cm^{-3} EB and photographed under UV light.

Molecular docking

Molecular docking studies were performed using Autodock/Vina program.[103] The PDB format of the complexes was obtained by converting its CIF file using Mercury software. The molecular geometry of complex **2** was fully optimized by DFT using the hybrid B3LYP approach and the LANL2DZ basis set.[104] Then, the structural parameters for **2** were converted to the PDB file. Two structures of B-DNA (1DNE, $d(CGCGATATCGCG)_2$ and 1DSC, $d(GAAGCTTC)_2$) were selected from the Protein Data Bank. The water molecules and the ligands were removed from 1DNE and 1DSC before performing docking calculations. The binding site was centered on the DNA and a grid box was created with 60 × 60 × 60 points and a 0.375 Å grid spacing in which almost the entire macromolecules were involved. For each docking calculation, 20 different posses were requested within the energy range of 2 kcal mol^{-1}. All other parameters were kept at their default values.

Antioxidant activity

The radical-scavenging activity of the complexes was measured using 2,2-diphenyl-2-picryl-hydrazyl (DPPH).[105,106] The solutions of the complexes in MeOH at different concentrations was mixed with a solution of DPPH in MeOH (0.1 mM, 2 mL) and the final volume was made up to 5 mL with double distilled water. The resulting solutions were stirred rigorously. The DPPH solution in methanol was used as a control and MeOH alone was used as a blank. The solutions were incubated at 37 ºC for 30 min in dark. The absorbance of the solutions was measured at 517 nm.

The total antioxidant activity of the complexes was studied using the 2,2'-azino-bis(3-ethylbenzthiazoline-6-sulfonic acid) (ABTS) cationic radical.[107] ABTS was dissolved in water to a 2 mM concentration and the $ABTS^{\bullet+}$ radical was produced by adding 0.2 mM potassium persulfate into the ABST solution. The resulting mixture was kept in the dark at room temperature for 12-16 h before use. The ABTS solution was diluted with MeOH to give an absorbance of 0.70 at 743 nm. The various concentrations of the solutions of the complexes in MeOH were added to 2 mL of the diluted ABTS cationic radical solution and the final volume was made up to 5 mL with double distilled water. Then, the absorbance reading was taken against MeOH at 15 min after the initial mixing.

All of the tests were run in triplicate, and the percentage of activity was calculated by using % radical activity = $[(A_0 - A_c)/A_0] \times 100$, where A_0 and A_c represent the absorbance in the absence and presence of the complexes, respectively. Ascorbic acid and butylated hydroxytoluene (BHT) were used as standards for the two tests. The 50% activity (IC_{50}) was calculated using the percentage of activity.

Cytotoxic activity assay (MTT)

Stock concentrations of cisplatin, carboplatin, oxaliplatin and complexes **1–6** were prepared in DMSO, while their final concentrations were prepared in the culture medium. For each

complex and anticancer drug, seven different concentrations ranging from 3.12 to 300 μM were used. The results represented the mean of two or three independent experiments run in triplicates.

Human carcinoma cell lines of MCF-7 (breast), HT-29 (colon) and DU-145 (prostate) were used, while PNT-1A (human prostatic epithelial cell) was used as normal cell.

The colon cell line (HT-29) was cultured in McCoy's medium supplemented with penicillin G (100 U/mL), streptomycin (100 μg/mL), L-glutamine, and 10% fetal calf serum at 37 °C in a humidified atmosphere containing 5% CO_2. The other cell cell lines were cultured in RPMI medium supplemented with penicillin G (100 U/mL), streptomycin (100 μg/mL), L-glutamine, and 10% fetal calf serum at 37 °C in a humidified atmosphere containing 5% CO_2.

The MTT cell viability assay [3-(4,5-dimethylthiazol-2-yl)-2,5-diphenyltetrazoliumbromide] was performed as follows. The cells were seeded in 200 μL culture medium in triplicates at a density of $5x10^3$ cells per well in a 96-well plate. Cells were treated with different concentrations of each complex for 48 h. Untreated cells were used as positive control for viability. MTT was supplied as a stock solution (5 mg/mL in PBS, pH 7.2) and sterile-filtered. At the end of the treatment period, 20 μL of MTT solution was added to each well. Following 4 h of incubation, 100 μL of solubilizing buffer (10% SDS dissolved in 0.01 N HCl) was added to each well. After 16 h incubation, the absorbance was determined by an ELISA plate reader at 594 nm as a read-out for cell viability. The cytotoxicity is mainly determined by the IC_{50} value (the dose inhibiting 50% of growth with respect to viability control) of each metal complex.

Acknowledgements

This work is a part of a research project 111T099. The authors are thankful to TUBITAK for the financial support given to the project. We also thank Dr. Murat Cengiz at Department of Pharmacology and Toxicology, Uludag University for the permission to use his laboratory for the electrophoresis work and Dr. S. D. Erim at Department of Medicinal Biochemistry of Uludag University for her assistance in cellular uptake experiments.

Notes and references

[a] Department of Chemistry, Faculty of Arts and Sciences, Uludag University, 16059 Bursa, Turkey. E-mail: vtyilmaz@uludag.edu.tr

[b] Department of Genetics, Faculty of Veterinary Medicine, Uludag University, 16059 Bursa, Turkey.

[c] Department of Chemistry, University of Aberdeen, Meston Walk, Aberdeen AB24 3UE, Scotland, UK.

[d] Department of Physics, Faculty of Arts and Sciences, Ondokuz Mayis University, 55159 Samsun, Turkey.

Electronic Supplementary Information (ESI) available: Stability of the complexes, interaction with DNA, molecular docking. See DOI: 10.1039/b000000x/

1. C. Orvig and M. J. Abrams, *Chem. Rev*., 1999, **99**, 2202.
2. C. S. Allardyce, A. Dorcier, C. Scolaro, and P. J. Dyson, *App. Organomet. Chem*., 2005, **19**, 1.
3. P. J. Dyson and G. Sava, *Dalton Trans*., 2006, **16**, 1929.
4. M. J. Hannon, *Pure Appl. Chem*., 2007, **79**, 2243.
5. K. B. Garbutcheon-Singh, M. P. Grant, B. W. Harper, A. M. Krause-Heuer, M. Manohar, N. Orkey and J. R. Aldrich-Wright, *Current Topics in Med. Chem*., 2011, **11**, 521.
6. P. Marques-Gallego, H. Dulk, J. Brouwer, H. Kooijman, A. L. Spek, O.Roubean, S. J. Teat and J. Reedijk, *Inorg. Chem*., 2008, **47**, 11171.
7. J. Reedijk, *Eur. J. Inorg. Chem*., 2009, **10**, 1303.
8. K. J. Barnham, M. I. Djuran, P. del Socorro-Murdoch, J. D. Ranford and P. J. Sadler, *Inorg. Chem*., 1996, **35**, 1065.
9. X. Wang, H. Li, X. Du, J. Harris, Z. Guo and H. Sun, *Chem. Sci*., 2012, **3**, 3206.
10. J. Zhao, S. Gou, Y. Sun, R. Yin and Z. Wang, *Chem. Eur. J*., 2012, **18**, 14276.
11. J. Zhao, S. Gou, Y. Sun, L. Fang and Z. Wang, *Inorg. Chem*., 2012, **51**, 10317.
12. Q. He, C. H. Liang and S. J. Lippard, *Proc. Natl. Acad. Sci. U. S. A*., 2000, **97**, 5768.
13. D. B. Zamble, Y. Mikata, C. H. Eng, K. E. Sandman and S. J. Lippard, *J. Inorg. Biochem*., 2002, **91**, 451.
14. A. H. Wang, J. Nathans, G. van der Marel, J. H. van Boom and A. Rich, *Nature*, 1978, **276**, 471.
15. H. Baruah, C.G. Barry and U. Bierbach, *Curr. Top. Med. Chem.* 2004, **4**, 1537.
16. Z. Ma, J. R. Choudhury, M. W. Wright, C. S. Day, G. Saluta, G. L. Kucera and U. Bierbach, *J. Med. Chem*. 2008, **51**, 7574.
17. H. -K. Liu and P. J. Sadler, *Acc. Chem. Res*., 2011, **44**, 349.
18. C. Icsel and V. T. Yilmaz, *DNA Cell Biol*., 2013, **32**, 165.
19. B. Onfelt, P. Lincoln and B. Nordén. *J. Am. Chem. Soc*., 2001, **123**, 3630.
20. A. C. G. Hotze, E. P. L. van der Geer, H. Kooijman, A. L. Spek, J. G. Haasnoot and J. Reedijk. *Eur. J. Inorg. Chem*., 2005, 2648.
21. S. Komeda, T. Moulaei, K. K. Woods, M. Chikuma, N. P. Farrell and L. D. Williams. *J. Am. Chem. Soc*., 2006, **128**, 16092.
22. A. Kar, *Medicinal Chemistry*, New Age International (P) Ltd. Publishers, New York, 2006, pp. 116-147.
23. J. J. L. Zwikker, *Pharm. Weekblad*, 1931, **68**, 975.
24. K. T. Mahmudova, M. N. Kopylovicha, A. M. Maharramov, M. M. Kurbanova, A. V. Gurbanov and A. J. L. Pombeiro, *Coord. Chem. Rev*., 2014, **265**, 1.
25. R. Faggiani, B. Lippert and C. J. L. Lock, *Inorg. Chem*., 1980, **19**, 295.
26. B. Lippert, *Inorg. Chem*., 1981, **20**, 4326.
27. G. Raudaschl-Sieber and B. Lippert, *Inorg. Chem*., 1985, **24**, 2426.
28. M. Höpp, A. Erxleben, I. Rombeck, and B. Lippert, *Inorg. Chem.*, 1996, **35**, 397.
29. M. Höpp, A. Erxleben, I. Rombeck, and B. Lippert, *Inorg. Chem.*, 1996, **35**, 6352.
30. J. Fawcett, W. Henderson, R. D. W. Kemmitt,D. R. Russell and A. Upreti, *J. Chem. Soc. Dalton Trans*., 1996, 1897.
31. N. Haque, PhD dissertation, Ludwig-Maximilians-Universität München, 2009.

32. I. M. Müller and D. Möller, *Angew. Chem. Int. Ed*., 2005, **44**, 2969.
33. V. T. Yilmaz, F. Yilmaz, H. Karakaya, O. Buyukgungor and W. T. A. Harrison, *Polyhedron*, 2006, **25**, 2829.
34. F. Yilmaz, V. T. Yilmaz, H. Karakaya and O. Buyukgungor, *Z. Naturforsch*, 2008, **63b**, 134.
35. M. S. Refat and N. M. El-Metwaly, *J. Mol. Struct*., 2011, **988**, 111.
36. M. M. Ibrahim, S. Al-Juaid, M. A. Mohamed and M. H. Yassin, *J. Coord. Chem*., 2012, **65**, 2957.
37. B. J. McCormick, E. N. Janes Jr., R. I. Kaplan, H. C. Clark and J. D. Ruddick, *Inorg. Synth*., 1972, **13**, 216.
38. G. T. Morgan and F. H. Burstall, *J. Chem. Soc*., 1934, 965.
39. M. J. Rauterkus, S. Fakih, C. Mock, I. Puscasu and B. Krebs, *Inorg. Chim. Acta*, 2003, **350**, 355.
40. D. Li, D. Liu, *Cryst. Res. Technol*., 2004, **39**, 359.
41. M. M. Mdleleni, J. S. Bridgewater, R. J. Watts and P. C. Ford, *Inorg. Chem*., 1995, **34**, 2334.
42. W. J. Geary, *Coord. Chem. Rev*., 1971, **7**, 81.
43. C. M. Santos, S. Cabrera, C. Rios-Luci, J. M. Padron, I. Lopez Solera, A. G. Quiroga, M. A. Medrano, C. Navarro-Ranninger and J. Aleman, *Dalton Trans*., 2013, **42**, 13343.
44. J. M. Herrera, F. Mendes, S. Gama, I. Santos, C. Navarro-Ranninger, S. Cabrera and A. G. Quiroga, *Inorg. Chem*., 2014, **53**, 12627.
45. W. Micklitz, J. Riede, B. Huber, G. Muller and B. Lippert, *Inorg. Chem*., 1988, **27** 1979.
46. W. Micklitz, W. S. Sheldrick and B. Lippert, *Inorg. Chem*., 1990, **29**, 211.
47. F. T. Ladipo, G. K. Anderson and N. P. Rath, *Organomet*., 1994, **13**, 4741.
48. M. Janka, G. K. Anderson and N. P. Rath, *Inorg. Chim. Acta*, 2004, **357**, 2339.
49. M. D. Santana, R. Garcia-Bueno, G. Garcia, G. Sanchez, J. Garcia, A. R. Kapdi, M. Naik, S. Pednekar, J. Perez, L. Garcia, E. Perez and J. L. Serrano, *Dalton Trans*., 2012, **41**, 3832.
50. E. C. Constable, A. M. W. C. Thompson, T. A. Leese, D. G. J. Reese and D. A. Tocher, *Inorg. Chim. Acta*, 1991, **182**, 93.
51. G. Sanchez, J. L. Serrano, M. A. Moral, J. Perez, E. Molins and G. Lopez, *Polyhedron*, 1999, **18**, 3057.
52. W. Lu, D. A. Vicic and J. K. Barton, *Inorg. Chem*., 2005, **44**, 7970.
53. A. Hazell, O. Simonsen and O. Wernberg, *Acta Cryst*., 1986, **C42**, 1707.
54. A. Rotondo, G. Bruno, M. Cusumano and E. Rotondo, *Inorg. Chim. Acta*, 2009, **362**, 4767.
55. R. S. Osborn and D. Rogers, *J. Chem. Soc. Dalton Trans*., 1974, 1002.
56. Y. -Q. Gong, Y. -F. Cheng, J. -M. Gu and X.-R. Hu, *Polyhedron*, 1997, **16**, 3743.
57. W. Henderson, A. G. Oliver, C. E. F. Rickard and L. J. Baker, *Inorg. Chim. Acta*, 1999, **292**, 260.
58. L. R. Falvello, R. Garde, E. M. Miqueleiz, M. Tom and E. P. Urriolabeitia, *Inorg. Chim. Acta*, 1997, **264**, 297.
59. A. M. Shemsi, B. El Ali, K. A. Ziq, M. Morsy, T. D. Keene, S. Decurtins and M. Fettouhi, *Inorg. Chem. Comm*., 2007, **10**, 1355.
60. E. J. Gao, H. X. Yin, M. C. Zhu, Y. G. Sun, X. F. Gu, Q. Wu and L. X. Ren, *J. Struct. Chem*., 2008, **49**, 1048.
61. E. Guney, V. T. Yilmaz and C. Kazak, *Polyhedron*, 2010, **29**, 1285.
62. Y. Wang, Y. Mizubayashi, M. Odoko and N. Okabe, *Acta Cryst*., 2005, **C61**, m67.
63. M. Yodoshi and N. Okabe, *Chem. Pharm. Bull*., 2008, **56**, 908.
64. B. Antonioli, D. J. Bray, J. K. Clegg, K. Gloe, K. Gloe, A. Jager, K. A. Jolliffe, O. Kataeva, L. F. Lindoy, P. J. Steel, C. J. Sumby and M. Wenzel, *Polyhedron*, 2008, **27**, 2889.
65. E. Guney, V. T. Yilmaz and O. Buyukgungor, *Inorg. Chim. Acta*, 2010, **363**, 2416.
66. C. Tu, X. Wu, Q. Liu, X. Wang, Q. Xu and Z. Guo, *Inorg. Chim. Acta*, 2004, **357**, 95.
67. R. Romeo, N. Nastasi, L. M. Scolaro, M. R. Plutino, A. Albinati and A. Macchioni, *Inorg. Chem*., 1998, **37**, 5460.
68. F. Yilmaz, V. T. Yilmaz, E. Soyer and O. Buyukgungor, *Inorg. Chim. Acta*, 2010, **363**, 3165.
69. V. T. Yilmaz, E. Soyer and O. Buyukgungor, *J. Organomet. Chem*., 2009, **694**, 3306.
70. A. M. Pyle, J. P. Rehmann, R. Meshoyrer, C. V. Kumar, N. J. Turro and J. K. Barton, *J. Am. Chem. Soc*., 1989, **111**, 3051.
71. M. Cusumano, M. L. Di Pietro, and A. Giannetto, *Inorg. Chem*., 1999, **38**, 1754.
72. J. -B. Lepecq and C. Paoletti, *J. Mol. Biol*., 1967, **27**, 87.
73. M. Cusumano, M. L. Di Pietro, A. Giannetto, F. Nicolo and E. Rotondo, *Inorg. Chem*., 1998, **37**, 563.
74. M. Lee, A. L. Rhodes, M. D. Wyatt, S. Forrow and J. A. Hartley, *Biochem*., 1993, **32**, 4237.
75. D. A. Barawkar and K. N. Ganesh, *Nucleic Acids Res*., 1995, **23**, 159.
76. R. Palchaudhuri and P. J. Hergenrother, *Curr. Opin. Biotechnol*., 2007, **18**, 497.
77. T. Afrati, A. A. Pantazaki, C. Dendrinou-Samara, C. Raptopoulou, A. Terzis and D. P. Kessissoglou, *Dalton Trans*., 2010, **39**, 765.
78. S. Anbu, M. Kandaswamy, S. Kamalraj, J. Muthumarry and B. Varghese, *Dalton Trans*., 2011, **40**, 7310.
79. O. Stern and M. Volmer, *Z. Phys*., 1919, **20**, 183.
80. R. Frank and H. Rau, *J. Phys. Chem*., 1983, **87**, 5181.
81. J. R. Lakowitcz, *Principles of Fluorescence Spectroscopy*, Plenum Press, New York, 1999, pp. 237–259.
82. G. Cohen and H. Eisenberg, *Biopolymers*, 1969, **8**, 45.
83. J. M. Kelly, A. B. Tossi, D. J. McConnell and C. OhUigin, *Nucleic Acids Res*., 1985, **13**, 6017.
84. D. Suh and J. B. Chaires, *Bioorg. Med. Chem*., 1995, **3**, 723.
85. R. Thomas, *Gene*, 1993, **135**, 77.
86. J. L. Mergny and L. Lacroix, *Oligonucleotides*, 2003, **13**, 515.
87. G. A. Neyhart, N. Grover, S. R. Smith, W. A. Kalsbeck, T. A. Fairley, M. Cory and H. H. Thorp, *J. Am. Chem. Soc*., 1993, **15**, 4423.
88. C. V. Kumar, E. H. A. Punzalan and W. B. Tan, *Tetrahedron*, 2000, **56**, 7027.
89. H. L. Wu, W. Y. Li, K. Miao, X. W. He and H. Liang, *Spectrosc Lett*., 2002, **35**, 781.
90. V. Rajendiran, M. Murali, E. Suresh, M. Palaniandavar, V. S. Periasamy and M. A. Akbarsha, *Dalton Trans*., 2008, 2157.
91. V. Rajendiran, M. Murali, E. Suresh, S. Shinka, K. Somasundaram and M. Palaniandavar, *Dalton Trans*., 2008, 148.
92. L. F. Chin, S. M. Kong, H. L. Seng, Y. L. Tiong, K. E. Neo, M. J. Maah, S. B. A. Khoo, M. Ahmad, T. S. A. Hor, H. B. Lee, S. L. San and C. H. Ng, *J. Biol. Inorg. Chem*., 2012, **17**, 1093.

93. E. Gallori, C. Vettori, E. Alessio, F. G. Vilchez, R. Vilaplana, P. Orioli, A. Casini and L. Messori, Arch. *Biochem. Biophys*., 2000, **376**, 156.
94. M. S. Puvvada, J. A. Hartley, T. C. Jenkins and D. E. Thurston, *Nucleic Acids Res*., 1993, **21**, 3671.
95. C. G. Ricci and P. A. Netz, *J. Chem. Inf. Model.*, 2009**, 49**, 1925.
96. J. Ancerewicz, E. Migliavacca, P. -A. Carrupt, B. Testa, F. Brée, R. Zini, J. -P. Tillement, S. Labidalle, D. Guyot, A. -M. Chauvet-Monges, A. Crevat and A. Le Ridant, *Free Radical Biol. Med*., 1998, **25**, 113.
97. F. Dimiza, A. N. Papadopoulos, V. Tangoulis, V. Psycharis, C. P. Raptopoulou, D. P. Kessissoglou and G. Psomas, *Dalton Trans*., 2010, **39**, 4517.
98. A. -R. Ghezzi, M. Aceto, C. Cassino, E. Gabano, D. Osella, *J. Inorg. Biochem*., 2004, **98**, 73.
99. J. Marmur, *J. Mol. Biol*., 1961, **3**, 208.
100. M. E. Reichman, S. A. Rice, C. A. Thomas and P. Doty, *J. Am. Chem. Soc*., 1954, **76**, 3047.
101. G. M. Sheldrick, *Acta Cryst*., 2008, **A64**, 112.
102. A. L. Spek, *J. Appl. Cryst*., 2003, **36**, 7.
103. O. Trott and A. J. Olson, *J. Comput. Chem*., 2010, **31**, 455.
104. A. D. Becke, *J. Chem. Phys*., 1993, **98**, 5648.
105. M. S. Blois, *Nature*, 1958, **29**, 1199.
106. K. Elizabeth and M. N. A. Rao, *Int. J. Pharma*., 1990, **58**, 237.
107. R. Re, N. Pellegrini, A. Proteggente, A. Pannala, M. Yang and C. R. Evans, *Free Radicals Bio. Med*., 1999, **26**, 1231.

